# Play with the ants to understand CASOS

Nicholas C. Georgantzas, Fordham University @ Lincoln Center, New York, NY 10023, USA
Tel.: (+212) 636-6216, ƒax: (+212) 765-5573, e-mail: georgantzas@fordham.edu

*Abstract*—The dynamics *complex, adaptive, self-organizing systems* (CASOS) produce often contradict the second law of thermodynamics. This paradox persists unless coupled to a system's macro level, where self-organizing agents act, is a micro level, where random processes increase *entropy*, i.e. uncertainty. Metaphorically speaking, the system's micro level permits overall system entropy to increase while sequestering its increase at the macro level, where *autopoiesis*, i.e. self-organization occurs. To render this metaphor precise, Parunak & Brueckner (2001) built an ant pheromone-driven CASOS simulation and measured Shannon's entropy at the macro (agent) and micro (pheromone) levels, showing an entropy-based view of autopoiesis. This essay presents a system dynamics model that replicates parts of Parunak & Brueckner's results and examines self-organization causally, as opposed to just measuring coincidental macro- and micro-level entropy. Despite its present inability to tag undifferentiated agents' individual attributes, the system dynamics method and software can help agent-system designers, managers and researchers understand exactly how CASOS' circular or feedback-loop relations produce nonlinear dynamics spontaneously out of their local interactions. Their distributed control leads positive feedback-loop relations to explosive growth, which ends when all dynamics has been absorbed into an attractor, leaving the system in a stable, negative feedback state.

*Keywords*: autopoiesis, entropy, loop polarity, pheromones, self-organization, strategy design, uncertainty

## Introduction

The pace at which business changes today no longer resembles some managers' internal models of reality. Consequently, full of anxiety, stress and uncertainty, they do not know how to act (Georgantzas & Acar 1995). Founder and CEO emeritus of VISA, Dee Hock (1998) sees three ways in which managers can respond:

*First*, they can try to impose their perception of reality on external circumstances to make reality behave the way it *should*—what many institutions try to do today. The *second* alternative is for managers to go into denial, refuse to think, insulate themselves from reality or create another reality they do understand. The *third* alternative requires that managers examine their internal models of reality and try to change them. This is difficult because it (a) questions one's whole identity and sense of value in the world, and (b) requires high-level learning. Yet, this is the only alternative that works.

The internal or mental model of almost everyone in the world today shows in the machine metaphors we utter: he's a big wheel, she went ballistic, he's got a screw loose, the group is ticking like a clock, we need to get in high gear, let's reengineer the organization, etc. All these are machine metaphors and analogies. But you would die if you reengineered your body according to them. Where would the CEO of your immune system and brain be?

Business leaders have built for years on Newton's mechanics principles, as if people were gears in a timepiece. And it worked, until modern life's speed of change and complexity began to overwhelm grand hierarchies, from the Soviet Union to the mainframe computer. The new framework for business is the biological world, where efficient actions produce robust results through *autopoietic*, i.e. self-organizing, adaptation (Zeleny 2000).

Nature helps discover alternatives to mechanical organization. Nature's system structures or processes explain the dynamics of living systems. Examples of such systems are human

learning and intelligence, organizational adaptation and development, and the historical evolution of business firms. *Complex, adaptive, self-organizing system* (CASOS) ideas help organizational change efforts, such as business process (re)design. Self-organization entails spontaneous system change, however, a constant evolution enabled by distributed control and triggered by *internal* variations. Consequently, for a firm to exist, adapt, survive and evolve, it must integrate its suppliers and customers, and collaborate with competitors—a huge chunk of its business environment.

A system is an organized group of interacting components working together for a purpose. Control over the system's behavior is either centralized in a distinct subsystem, or distributed among its components. Distributed control enables complex, adaptive, self-organizing systems to create globally coherent behavior patterns, i.e., dynamics, spontaneously, through locally interacting components (Georgantzas 2001a).

Intrigued by CASOS outcomes, business researchers and practitioners eagerly adopt the principles underlying CASOS. Evidently, spontaneous self-organization business applications fall into two clear-cut categories. The first is *metaphorical* and the second *computational.*

On their own, metaphors describe outcomes only—neither why nor how CASOS processes work, and thereby treat spontaneous autopoiesis as a black box. Much more conducive to effective decision making through high-level learning, the purpose of computation is to make the black box transparent; to understand why and exactly how autopoiesis generates magnificent patterns; how CASOS structures produce their intricate dynamics.

The metaphorical treatment with examples linking business to nature captures the imagination of business managers and scholars, but demands maintaining a tolerant yet sceptical view of its connotations. Benefiting from CASOS requires preserving their rigor through simulation modeling, to avoid either being unduly metaphorical, i.e. hand waving, or blindly trying to import theories from the physical and life sciences to business. One benefit from computing *autopoietic* dynamics is to understand contemporary business phenomena, such as the emerging virtual enterprise networks (VENs) with their autopoietic industry value chains. Through their *poiesis-bonding-degradation* cycles, VENs self-organize spontaneously into *organizationally closed* and *thermodynamically open* markets (Georgantzas 2001b).

CASOS examples of human culture and insect colonies show that individual autonomy can be compatible with global order. Widespread human experience warns, however, that building systems that combine individual autonomy and global order is not a trivial task. At the root of the ubiquity of disorganizing tendencies, CASOS researchers see the *second law of thermodynamics*, which says that systems tend to run down from order to disorder, from *enthalpy* (energy) to entropy (Heylighen 1999). Adding energy to a system can overcome the second law of thermodynamics and thereby increase order, but how one adds energy is critical. Gasoline added to construction equipment, for example, can help construct a building out of steel and concrete, but the same gasoline in a bomb reduces the building back to a mass of steel and concrete (Parunak & Brueckner 2001).

The relation, however, between multi-agent CASOS and thermodynamics, such as the second law, provides quantitative, analytical guidelines for designing multi-agent systems. Parunak & Brueckner's (2001) ant pheromone-driven simulation shows how these ideas can be used to measure the behavior of multi-agent CASOS. Kugler & Turvey (1987), who inspired Parunak & Brueckner work, argue that to contain disorder in a multi-agent system one must couple that system to another in which disorder increases. To render this metaphor precise, Parunak & Brueckner (2001) simulate an ant pheromone-driven CASOS and measure Shannon's statistical

entropy (Shannon & Weaver 1949) at the macro (ant agent) and micro (pheromone molecule) levels, showing an entropy-based view of autopoiesis.

After the *CASOS overview* below, the *pheromone-driven CASOS* section reviews Kugler & Turvey's (1987) and Parunak & Brueckner's (2001) work. Then, the system dynamics *model-description* section shows a model that replicates parts of Parunak & Brueckner's ant pheromone-driven CASOS dynamics in the *experimental results* section. Using system dynamics to play with the ants and to understand CASOS, however, also allows looking at autopoiesis causally, as opposed to merely looking at coincidental macro- and micro-level entropy measures. The *beyond entropy: feedback-loop structure* section shows how, despite its present inability to tag undifferentiated agents' individual attributes, system dynamics helps to understand exactly how CASOS' circular or feedback-loop relations produce nonlinear dynamics spontaneously out of local interactions. As *shifting loop polarity* (slp) determines system behavior (Richardson 1995), distributed control leads positive feedback-loop relations to explosive growth, which ends when all dynamics has been absorbed into an attractor, leaving the system in a stable, negative feedback state. The *conclusion* section briefly outlines model variants and the implications of moving CASOS from the forefront of business research to policy and strategy in practice.

## CASOS overview

Complex, adaptive, self-organizing systems (CASOS) have grown out of disparate fields, including physics, chemistry, biology, cybernetics, computer modeling, and economics. This has led to a fragmented approach, with many different concepts, terms and methods applied to *seemingly* different types of systems. A fundamental concepts and principles core has emerged, however, applicable to all self-organizing systems, from simple magnets and crystals to brains and societies (Scholl 2001). Salient CASOS characteristics include: (a) bifurcations and symmetry breaking, (b) distributed control, (c) far from equilibrium dynamics, (d) global order from local interactions, (e) non-linearity and feedback, (f) organizational closure, hierarchy and emergence, and (g) robustness and resilience (Heylighen 1999).

Nature's spontaneous emergence of SOS dynamics is easy to see both in the laboratory and in our day-to-day world. A simple example is crystallization, the appearance of beautifully symmetric patterns of dense matter in solutions of randomly moving molecules. Other examples are certain chemical reactions, such as the *Brusselator* or the Belouzov-Zhabotinsky (BZ) reaction, where it suffices to pump ingredients into a solution in order to see pulsating color spirals (Zhabotinsky 1973).

The oscillatory BZ reaction dynamics has implications not only for chemistry but also for biological systems. It contradicts the second law of thermodynamics and shows that, under certain conditions, homogeneous closed systems oscillate spontaneously around their expected stationary states when approaching equilibrium. Reconciling CASOS with thermodynamics is simple in the crystallization case. Molecules fixed within a crystalline structure pass on their energy to the liquid they were dissolved. The increase in the liquid's entropy sequesters further increases in the crystals' entropy. The entropy of the whole system, liquid and crystals together, effectively increases. The solution is less obvious, however, when CASOS do not reach equilibrium. Belgian thermodynamicist Ilya Prigogine received a Nobel Prize for his work on this problem. He and his colleagues at the Brussels school of thermodynamics have been studying *dissipative structures* (Prigogine & Strengers 1984).

Like the BZ reaction, dissipative structures are autopoietic. Necessarily open systems, energy and/or matter flow through them. A system continuously generates entropy that is actively dissipated or exported out. Systems manage to increase their own organization at the expense of

order in the environment. They circumvent the second law of thermodynamics by getting rid of excess entropy. Living organisms show dissipative spontaneous dynamics. Plants and animals take in energy and matter in a low entropy form as light or food. They export it back in a high entropy form, i.e. waste products. This allows them to reduce their internal entropy, thus counteracting the degradation implied by the second law.

Exporting entropy does not explain how or why self-organization takes place in nonlinear systems far from thermodynamic equilibria. Fortunately, autonomous systems in *cybernetics* complement the thermodynamicists' observations. Independently of its type or composition, an autonomous system always evolves toward a state of equilibrium (attractor). This reduces uncertainty about the system's state and, thereby, statistical entropy. System parts mutually adapt to the resulting equilibrium. Paradoxically, the larger the random perturbations (noise) that affect a system, the more quickly it will self-organize (produce order).

The idea is simple: the more widely a system moves through its state space, the faster it ends up in an attractor. No attractor is reached and no self-organization takes place if a system stays put. Generally, nonlinear systems have several attractors. An attractor is either a stable equilibrium, i.e. a fixed point or a limit cycle, and thereby nonchaotic, or an unstable equilibrium, i.e. aperiodic or chaotic. When caught in between attractors, a system is in a chance variation, called *fluctuation* in thermodynamics, which pushes it into either one of its attractors (Prigogine & Strengers 1984).

Since the 1950s and 1960s, when CASOS were first studied in thermodynamics and cybernetics, many examples and applications have been discovered. Prigogine generalized his observations to argue for a new scientific worldview. Instead of the Newtonian reduction to a static *being* framework, he sees the universe as an irreversible *becoming*, which endlessly generates novelty.

Cyberneticians apply self-organization to the mechanisms of mind, to understand how the brain constructs mental models without relying on outside instruction. A practical application is neural networks, simplified computer models of how the neurons in our brain interact. Unlike the central reasoning control used in artificial intelligence (AI), distributed control rules a neural network (NN). All neurons are connected directly or indirectly with each other, but none is in control. Together, they manage to make sense, however, out of complex input patterns.

Laser light is another CASOS example. Atoms or molecules excited by an input of energy emit the surplus energy as photons, normally at random moments in random directions. The result is ordinary, diffused light. Under certain conditions, however, the molecules become synchronized, emitting the same photons at the same time in the same direction. The result is an exceptionally coherent, focused beam of light.

Plants and animals provide more examples of autopoietic behavior. Aspen groves, shoals of fish and termite towers are magnificent CASOS examples in nature. An aspen grove in Utah, for example, is the largest known living organism on earth. Each tree is connected to all others by the same underground root system—one vast connection (Wheatley 1996).

Flocks of birds, gangs of elk, herds of sheep, shoals of fish and swarms of bees react in similar ways. When avoiding danger or changing course, they generally move together in an elegantly synchronized manner. Sometimes, the flock or shoal behaves as if it were a single animal. There is *no* head fish or bird leader, however, that tells others how to move. Computer simulations reproduce this behavior by letting individuals interact according to a few simple rules, such as keeping a minimum distance from others and following the average direction of neighbours' moves. A global coherent pattern emerges out of local interactions.

Similarly, the twenty-foot termite towers in the Australian savannah are the result of distributed control. Each termite colony is a magnificent example self-organization, producing intricate towers from the *seemingly* random movements of many individuals. Relative to the size of their builders, termite towers are the tallest structures on Earth (Wheatley 1996).

*Metaphorical CASOS applications*

Nature helps managers willing to re-examine and to change their internal models of reality. As employees pursue their daily routines, changed managers encourage them to experiment, to make messes, to seek information and assistance in search of new ways to keep the company mission alive. Meanwhile, they create new streams of performance data so everyone can see what works. Unpredictable new structures and flows take shape through time, success building on success. Whether because of financial or other stakes, employees display boundless new eagerness for the work they control. Instead of driving ambiguity and instability out, managers who adhere to nature embrace them both.

CASOS principles won't succumb, however, to program-of-the-month syndrome because self-organizing adaptation is a ceaseless process in a real-time world of global business, with technologies, markets and relationships emerging and disappearing amid a fury of constant communication. And it recognizes the best of the baby-boomer culture and the detachment of Generation X. Naturally, some firms could be engulfed by the chaos they create but, so far, Petzinger (1997) sees nothing but success stories to report. Are CASOS the wave of the future, he asks, or are we all washed up?

Since the 1980s, several well-articulated and well-received books in the business literature advocate the study of organizations from an autopoietic systems view. For example, Morgan (1993) argues that the metaphor of organizations as a self-organizing, self-producing system offers powerful conceptual tools to examine organizations in flux. Equally fascinated by CASOS *connectedness* and *wholeness*, Senge et al. (1994) describe organizations as complex nonlinear systems, directed by charismatic leaders who intervene at critical leverage points.

Wheatley (1996) continues this advocacy about organizations as autopoietic systems by conveying the pleasure of sensing a new way of thinking about organizations. She acknowledges the danger in playing with science metaphors, but she also argues that all science is metaphor. Turning science back to anthropomorphic mythology, Wheatley reduces CASOS to mere images and uses their outcomes to define consciousness.

These authors and their followers love to metaphorically re-conceptualize organizations as dynamic, chaotic, non-linear systems, with self-similar structures, given to sudden disruptive changes, often triggered by small, seemingly random actions. They offer illustrative anecdotes of organizational activities and structures that appear to bear out CASOS characteristics. No matter how breathtaking, however, anecdotes hardly make up empirical evidence. Anecdotes and images are just metaphorical attempts to *imaginize* organizations (Morgan 1993).

The history of, and reaction to, earlier scientific metaphors suggest that disillusionment sets in when the public tires of the metaphor and the research community fails to see formalized intellectual advances. Even if hidden among wild exaggerations are important kernels of useful knowledge. This time around, however, *simulation modeling* holds out the promise that disillusionment can be pre-empted, or at least delayed (Turner 1997).

*Computational CASOS applications*

Complexity theory and the exponential increase in computational power make simulation modeling a critical fifth tool in addition to the four tools used in science: observation, logi-

cal/mathematical analysis, hypothesis testing and experiment (Turner 1997). Simulation modeling permits researchers and practitioners in a variety of disciplines to examine the aggregate, dynamic and emergent implications of multiple nonlinear generative mechanisms.

Swarms are but one of the many autopoietic systems studied through simulation modeling. Inexpensive and powerful computers make it possible to model and explore highly complex systems. Simulation modeling helps the *Santa Fe Institute* researchers in New Mexico study multi-agent CASOS that change constantly, both autonomously and in interaction with their environment.

Typical examples are ecosystems, where different species compete or cooperate while interacting in their shared environment. By generalizing the mechanisms through which biological organisms adapt, Holland (1997) founded the theory of *genetic algorithms*. This approach to computer problem solving relies on the mutation and recombination of partial solutions, and the selective reproduction of the most *fit* new combinations. By letting units that undergo variation and selection interact through signals or *resources*, Holland extended simulation modeling to cognitive, ecological and economic systems.

Markets are good CASOS examples, where producers compete and exchange money and goods with consumers. Although markets are highly chaotic, nonlinear systems, they usually reach equilibria, attractors that satisfy changing and conflicting customer demands. The failure of communism shows that markets' distributed control is more effective at organizing the economy than a centrally controlled system. CASOS computer simulations corroborate what Adam Smith, the father of economics, called *the invisible hand* (Sterman 2000, pp. 169-177).

Biologist Stuart Kauffman (1995) also studies the development of organisms and ecosystems. His simulation models show how networks of mutually activating or inhibiting genes differentiate organs and tissues during embryological development. Complex networks of chemical reactions self-organize into autocatalytic cycles, the precursors of life. CASOS develop autonomously and natural selection helps them adapt to variable environments.

Holland's and Kauffman's work provides essential inspiration for the new discipline of *artificial life*. This approach, initiated by Chris Langton, successfully builds computer programs that mimic lifelike properties, such as reproduction, sexuality, swarming, co-evolution and arms races between predator and prey.

Simulation modeling is also the chief catalyst for *chaos theory*. Using a deterministic simulation model of a weather system, MIT meteorologist Edward Lorenz (1963) discovered that even the most minuscule of changes cause drastic alterations in weather. That effect defied both intuition and what meteorologists had previously understood about their science. Intrigued by Lorenz's puzzle, scientists from different fields are experimenting with simulation models, only to discover similar dynamics. Yoshisuke Ueda (1992), for example, found a strange attractor in Duffing's system. The fundamental insight that minute changes can lead to large deviations in the behavior of a natural system has inaugurated a radical shift in how scientists see the world. For all practical purposes, the dynamics of even relatively simple systems is unpredictable. This is the *butterfly effect* that Ormerod describes in his 1999 book *Butterfly Economics*.

This does not mean that chaotic systems do not exhibit any patterns. While the idea of unpredictability is counterintuitive, chaos theory's *second* basic insight is even more so: behavior patterns do lurk beneath the *seemingly* random behavior of systems. Chaotic systems do not end up just anywhere. Certain paths show distributed intelligence or control.

Like biologists who are simulating cells that arrange themselves into immune systems, economists are simulating the limited actions of individual buyers and sellers that form complex

markets, industries and economies. Jay W. Forrester (1958) was the first to apply the computational principles of cybernetics to industrial systems.

Forrester's initial work in industrial systems has been subsequently broadened to include other social and economic systems and is becoming the field of *system dynamics* (Sterman 2000). Relying on the computer, system dynamics provides a coherent method for solving business, economic and social problems, particularly when chaotic attractors are involved. See for example the work of Erik Mosekilde and other system dynamics colleagues in the *System Dynamics Review: Special Issue on Chaos* (Richardson & Andersen 1988). A prerequisite for systems thinking, system dynamics simulation is the basis of this essay's CASOS model.

**Pheromone-driven CASOS**

In the context of biomechanical systems, Kugler & Turvey (1987) claim that CASOS can be reconciled with the second-law tendencies if a system includes coupled levels of dynamic activity. Purposeful, autopoietic behavior occurs at the macro level. By itself, such behavior would contradict the second law. The system includes a micro level, however, whose dynamics generate increasing disorder in the system as a whole through time. Crucially, the macro level is coupled to the micro level. To make Kugler & Turvey's metaphor precise, Parunak & Brueckner (2001) simulate an ant pheromone-driven CASOS, study its dynamics and comment on the legitimacy of reconciling information entropy with thermodynamic entropy (Hayes 1999).

Autopoietic insect colonies, such as the construction of minimal spanning tree networks among nests and food sources by ants, or the erection of multi-storied structures with regularly spaced pillars and floors by tropical termites, are good examples of pheromone-driven CASOS (Parunak 1997). Pheromones are scent markers that insects use in two ways. *First*, they deposit pheromones in the environment to record their state. A foraging ant, for example, just emerging from the nest in search of food deposits nest pheromones, while an ant that has found food and is carrying it will deposit food pheromones. *Second*, they orient their movements to the pheromone grids. In the foraging ants case, those seeking food climb the food pheromone grid, while those carrying food climb the nest pheromone grid. The most realistic models of the ants' pheromone-climbing behavior incorporate a stochastic element in their movement. That is, they do not follow any grid deterministically, but use its strength to weigh a roulette wheel from which they determine their movement. The environment in which ants deposit pheromones plays a critical role in such a system. It is active, as opposed to passive, and performs three information-processing functions with the pheromones (Table 1).

Table 1 Information-processing functions of the pheromone environment (adapted from Parunak & Brueckner 2001)

| # | *Function* | *Description* |
|---|---|---|
| 1 | Aggregation | The environment aggregates deposits of the same pheromone flavor from different ants, providing a form of data fusion across multiple agents at different times, based on their traversal of a common location. |
| 2 | Evaporation | The environment evaporates pheromones through time to forget obsolete information. This is a novel approach to truth maintenance. Conventional knowledge bases remember every assertion unless there is cause to retract it, and execute truth maintenance processes to detect and resolve the conflicts that result when inconsistent assertions coexist. Insect systems forget every assertion unless it is regularly reinforced. |
| 3 | Information Dissemination | Evaporation provides a third function, that of disseminating information from the location at which it was deposited to nearby locations. An ant does not have to stumble across the exact location at which pheromone was deposited in order to access the information it represents, but can sense the direction from its current location to the pheromone deposit in the form of the grid of evaporated pheromone molecules. |

Departing from classical views of agent organization, Fig. 1 shows the interplay among these processes. Classically, agents perceive one another directly, reason about their perception and then take rational action. In Kugler & Turvey's (1987) model, however, agents change their environment through their actions, i.e. by depositing pheromones, a process known as *stigmergy*. The environment in turn mediates autopoiesis through processes that generate structures the agents perceive, thus permitting ordered behavior at the agent or macro level. At the same time, these processes increase disorder at the micro level, so that the system as a whole becomes less ordered through time.

Figure 1
A pheromone-driven CASOS

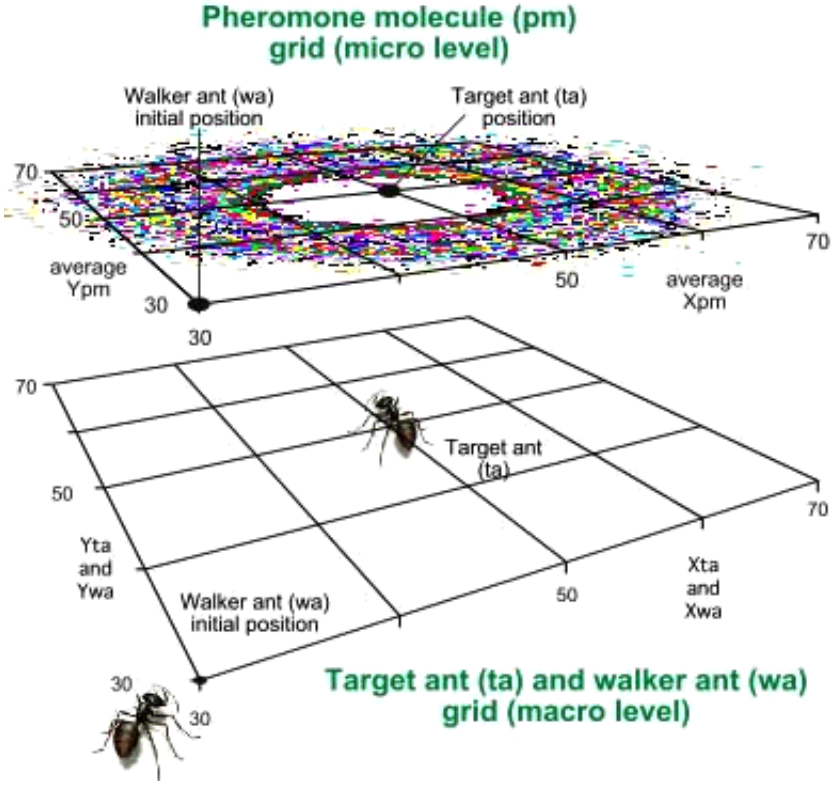


Ants and their movements constitute the macro level of the system, while pheromone molecules constitute the micro level (Fig. 1). As they move, the ants increase disorder at the macro level, which is coupled to the micro level, where pheromone molecules move and evaporate under Brownian motion, resulting in an overwhelming growth in disorder. Consistent with second law of thermodynamics, the disorder of the overall system increases in spite of the emergence of autopoiesis or self-organizing order at the macro level.

Synthetic pheromone researchers draw directly on autopoiesis, but its ideas apply broadly. In multi-commodity markets, for example, agents follow economic indicators generated by a myriad of individual transactions, and self-organization in the demand and supply of a particular commodity is supported by an environment that distributes resources based on other transactions in the system. The movement of currency in such a system provides similar functions to those of pheromones in insect systems. Coupling ordered and disordered systems is ubiquitous in robust CASOS, and the lack of such a coupling correlates with strategy designs that do not meet their designers' expectations for emergent autopoietic cohesiveness (Parunak & Brueckner 2000).

Parunak & Brueckner (2001) experiment with these ideas and measure Shannon's information entropy at the macro (agent) and micro (pheromone molecule) levels, thereby showing an entropy-based view of autopoiesis. Following Boltzmann's and von Neumann's work on statistical mechanics, Shannon defined information entropy as:

$$U = -k\sum_{i=1}^{n} p_i \log p_i, \qquad (1)$$

where $i$ ranges over all possible outcomes $n$, $p_i$ is the probability of finding an agent in state $i$, and $k$ is a positive constant (Shannon & Weaver 1949). Many years later Shannon said:

> My greatest concern was what to call it. I thought of calling it 'information', but the word was overly used, so I decided to call it 'uncertainty'. When I discussed it with John von Neumann, he had a better idea. Von Neumann told me: 'You should call it entropy, for two reasons. In the first place your uncertainty function has been used in statistical mechanics under that name, so it already has a name. In the second place, and more importantly, nobody knows what entropy really is, so in a debate you will always have the advantage (Tribus & McIrvine 1971).

The following section presents a system dynamics model that replicates parts of Parunak & Brueckner's ant pheromone-driven CASOS dynamics in the *experimental results* section. Because *nobody knows what entropy really is*, however, the model computes agent location uncertainty as opposed to Parunak & Brueckner's (2001) system location entropy. Moreover, unlike Parunak & Brueckner's walker ants who always spin a roulette for every step they take, the model cleanly separates the walkers' unguided, random motion from their pheromone-guided, deterministic motion.

**Model description**

Figure 1 shows two agents, one fixed and one mobile, who desire to be together. Neither agent knows the location of the other. If only it knew where to go, the mobile agent or walker ant (wa) would travel to the destination of the stationary one. The stationary agent or target ant (ta) deposits pheromone molecules at its location. As pheromone molecules (pm) diffuse through the environment, they create the micro-level pm grid that walker ants can follow. Figure 2 shows the model's target ant (ta) sector and Table 2 the corresponding algebra.

The target ant (ta) remains stationary at its (50, 50) location (Eqs 2.1.1 and 2.2.1) as long as its on\off switch equals zero (Eq. 2.5). If the switch equals one, however, then ta will move. First, it will compute a random angle, i.e. random ta $\partial \in [0, 2\pi]$ (2.6), relative to its current position. Then, as the graphical table function (gtf) of Fig. 2 and Table 2 (2.7) show, it will take a step in the resulting direction, once every five cycles of the simulation.

Parunak & Brueckner's (2001) ta never turns mobile, but making it so affects the macro- and micro-level agent location uncertainty. When ta moves, depending on its random heading and position, the random Xta change (2.3) and random Yta change (2.4) flows either increase or decrease the Xta (2.1) and Yta (2.2) stocks, respectively, one step every five time (t) units. Whether stationary or mobile, ta always deposits one pheromone molecule (pm) at its current location (Fig. 3 and 3.4, Table 3), whatever that might be. Like the walker and target ant agents, each pm agent also moves by computing a random angle, i.e. random pm $\partial \in [0, 2\pi]$ (3.16), relative to its current position.

Each pm agent then takes a step in the resulting direction, every cycle of the simulation (3.16, Table 3). Both pheromone molecules and walker ants can find themselves at any real-valued (X, Y) location on their respective grids (Fig. 1). Pheromone molecules move, however,

every cycle of the simulation with a pm step = 2 (3.15), while ants take only one step every five cycles. Altogether then, pheromone molecules move ten times faster than ant agents do.

Figure 2
The target ant (ta) sector (macro level)

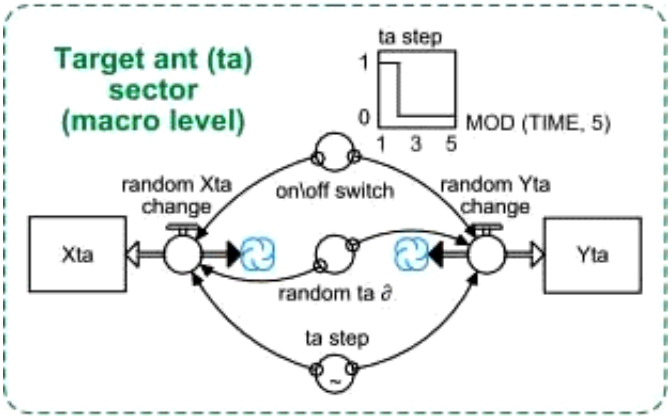


Table 2 Target ant (ta) sector (macro level) equations

| *Level or state variables (stocks)* | | *Eq. #* |
|---|---|---|
| Xta(t) = Xta(t - dt) + (random Xta change) * dt | | (2.1) |
| INIT Xta = 50 {unit = step} | ( t = TIME and dt = computation interval ) | (2.1.1) |
| Yta(t) = Yta(t - dt) + (random Yta change) * dt | | (2.2) |
| INIT Yta = 50 {unit = step} | | (2.2.1) |
| *Rate variables (flows)* | | |
| random Xta change = COS (random ta ∂) * ta step * on\off switch {unit = step/t} | | (2.3) |
| random Yta change = SIN (random ta ∂) * ta step * on\off switch {unit = step/t} | | (2.4) |
| *Auxiliary variables and constants (converters)* | | |
| on\off switch = 0 {0 = stationary ta and 1 = mobile ta; unit = dimensionless} | | (2.5) |
| random ta ∂ = RANDOM (0, 2*PI) {unit = radian} | | (2.6) |
| ta step = GRAPH(MOD (TIME, 5)) {unit = step} | | (2.7) |
| (1.00, 1.00), (2.00, 0.00), (3.00, 0.00), (4.00, 0.00), (5.00, 0.00) | | |

As Table 1 suggests, the environment aggregates pm deposits into the Pheromone Molecules stock (Fig. 3 and 3.1). These evaporate (3.5) randomly, however, depending on their time to evaporate ∈ [10, 40] (3.17). Parunak & Brueckner (2001) have their pm agents fall off their respective grid when they reach its edge. But the pm evaporation outflow of 3.5 renders an equally realistic implementation of the pm environment's evaporation function (Table 1).

Depending on aggregated Pheromone Molecules' random heading and position, the random Xpm change (3.7) and random Ypm change (3.9) flows either increase or decrease the Xpm (3.2) and Ypm (3.3) stocks, respectively, one step at a time (t). Each freshly deposited pm agent biases these stocks, however, towards the target ant (ta) agent's location, through the biased Xpm change (3.6) and biased Ypm change (3.10) flows, respectively. Lastly, for each pm agent that evaporates, the evaporation caused Xpm change (3.8) and evaporation caused Ypm change (3.11) flows subtract the average Xpm (3.12) and average Ypm (13) coordinate from the Xpm (3.2) and Ypm (3.3) stocks, respectively.

The pm micro-level sector stocks initialize automatically (Eqs 3.1.1–3.3.1). This allows playing with different pm parameters, such as pm production (3.4) and time to evaporate (3.17).

Back to the macro level (Fig. 4 and Table 4). While the ta (if mobile) and pm agents choose a heading for their next step from a uniform distribution, thereby executing an unbiased random

walk, the walker ant (wa) computes its heading from two inputs. Either it executes an unbiased random walk too, or it generates a vector from its current location to the average pm location.

Figure 3
The pheromone molecule (pm) sector (micro level)

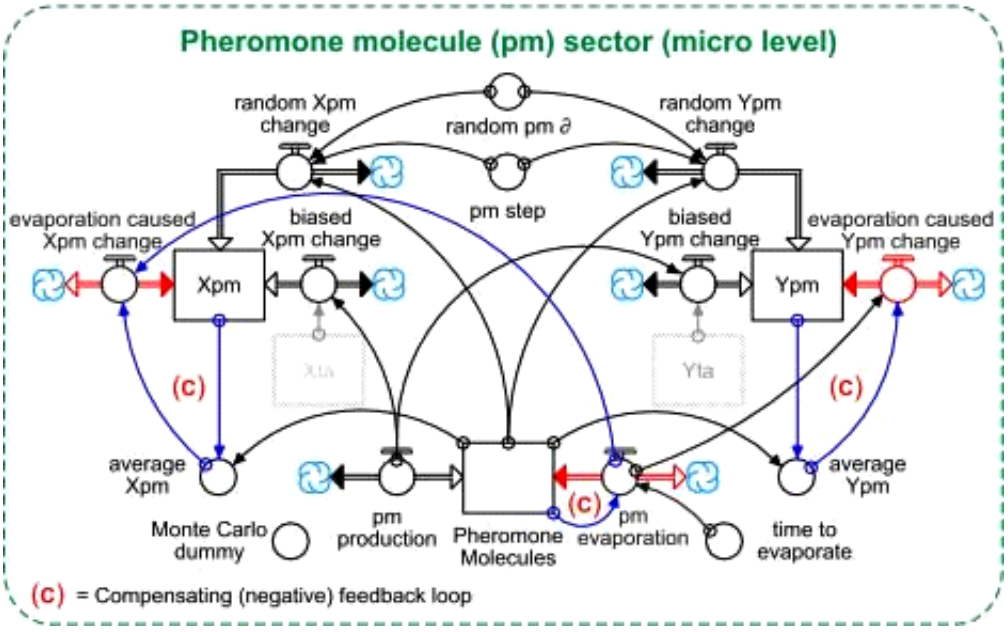


Table 3 Pheromone molecule (pm) sector (micro level) equations

| Level or state variables (stocks) | Eq. # |
|---|---|
| Pheromone Molecules(t) = Pheromone Molecules(t - dt) + (pm production - pm evaporation) * dt | (3.1) |
| INIT Pheromone Molecules = time to evaporate * pm production {unit = pm} | (3.1.1) |
| Xpm(t) = Xpm(t - dt) + (biased Xpm change + random Xpm change - evaporation caused Xpm change) * dt | (3.2) |
| INIT Xpm = Pheromone Molecules * Xta {unit = pm * step} | (3.2.1) |
| Ypm(t) = Ypm(t - dt) + (random Ypm change + biased Ypm change - evaporation caused Ypm change) * dt | (3.3) |
| INIT Ypm = Pheromone Molecules * Xta {unit = pm * step} | (3.3.1) |
| **Rate variables (flows)** | |
| pm production = 1 {unit = pm / t} | (3.4) |
| pm evaporation = Pheromone Molecules / time to evaporate {unit = pm / t} | (3.5) |
| biased Xpm change = pm production * Xta {unit = pm * step / t} | (3.6) |
| random Xpm change = (COS(random pm ∂) * pm step) * Pheromone Molecules {unit = pm * step / t} | (3.7) |
| evaporation caused Xpm change = average Xpm * pm evaporation {unit = pm * step / t} | (3.8) |
| random Ypm change = (SIN(random pm ∂) * pm step) * Pheromone Molecules {unit = pm * step / t} | (3.9) |
| biased Ypm change = pm production * Yta {unit = pm * step / t} | (3.10) |
| evaporation caused Ypm change = average Ypm * pm evaporation {unit = pm * step / t} | (3.11) |
| **Auxiliary variables and constants (converters)** | |
| average Xpm = Xpm / Pheromone Molecules {unit = step} | (3.12) |
| average Ypm = Ypm / Pheromone Molecules {unit = step} | (3.13) |
| Monte Carlo Dummy = 1 {unit = dimensionless} | (3.14) |
| pm step = 2 {unit = step} ( t = TIME and dt = computation interval ) | (3.15) |
| random pm ∂ = RANDOM (0, 2 * PI) {unit = radian} | (3.16) |
| time to evaporate = RANDOM (10, 40) {unit = t} | (3.17) |

It all depends on the wa radius parameter (4.11), or Parunak & Brueckner's (2001) r. If the walker ant's distance (4.9) from the average pm location is strictly larger than r = 25, then wa

executes an unbiased random walk. First, it computes a random angle, i.e. random wa ∂ Œ [0, 2p] (4.10), relative to its current position. It then takes a step in the resulting direction, once every five cycles of the simulation, as the gtf of Fig. 4 and Table 4 (Eq. 4.12) show. In this case, depending on wa's random heading and position, the random Xwa change (4.3) and random Ywa change (4.5) flows either increase or decrease the Xwa (4.1) and Ywa (4.2) stocks, respectively, one step every five time (t) units.

Figure 4
The walker ant (wa) sector (macro level)

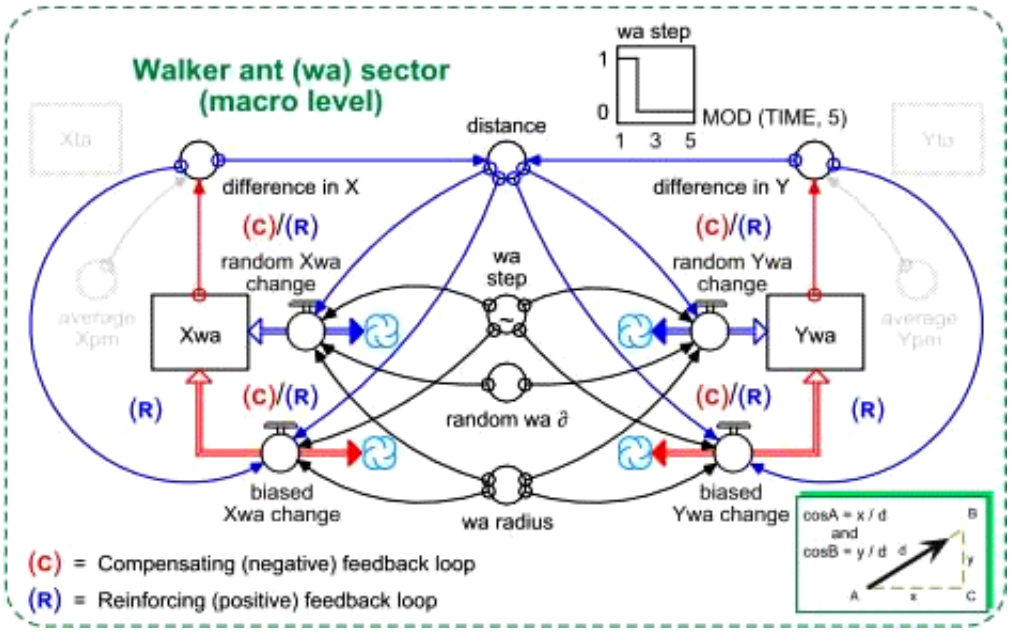


Table 4 Walker ant (wa) sector (macro level) equations

| *Level or state variables (stocks)* | *Eq. #* |
|---|---|
| Xwa(t) = Xwa(t - dt) + (random Xwa change + biased Xwa change) * dt | (4.1) |
| INIT Xwa = 30 {unit = step} | (4.1.1) |
| Ywa(t) = Ywa(t - dt) + (random Ywa change + biased Ywa change) * dt | (4.2) |
| INIT Ywa = 30 {unit = step} | (4.2.1) |
| *Rate variables (flows)* | |
| random Xwa change = IF (distance > wa radius) THEN (COS (random wa ∂) * wa step) ELSE (0) {unit = step / t} | (4.3) |
| biased Xwa change = IF (distance <= wa radius) THEN ((difference in X / distance) * wa step) ELSE (0) {unit = step / t} | (4.4) |
| random Ywa change = IF (distance > wa radius) THEN (SIN (random wa ∂) * wa step) ELSE (0) {unit = step / t} | (4.5) |
| biased Ywa change = IF (distance <= wa radius) THEN ((difference in Y / distance) * wa step) ELSE (0) {unit = step / t} | (4.6) |
| *Auxiliary variables and constants (converters)* | |
| difference in X = average Xpm - Xwa {unit = step} | (4.7) |
| difference in Y = average Ypm - Ywa {unit = step} | (4.8) |
| distance = SQRT((difference in X^2) + (difference in Y^2)) {unit = step} | (4.9) |
| random wa ∂ = RANDOM (0, 2*PI) {unit = radian} | (4.10) |
| wa radius = 25 {Parunak & Brueckner's (2001) ρ; unit = step} | (4.11) |
| wa step = GRAPH(MOD (TIME, 5) {unit = step}) (1.00, 1.00), (2.00, 0.00), (3.00, 0.00), (4.00, 0.00), (5.00, 0.00) | (4.12) |

If, however, wa's distance from the average pm location is less than or equal to $\rho = 25$, then the walker ant climbs the pheromone molecule grid. That is, it computes a vector from its current location to the average pm location. Depending on this vector's magnitude (see insert on lower right of Fig. 4), the biased Xwa change (4.4) and biased Ywa change (4.4) flows either increase or decrease the Xwa (4.1) and Ywa (4.2) stocks, respectively, every five time (t) units.

Directional change in these two flows depends on the sign of the difference in X (4.7) and difference in Y (4.8), respectively. It is inside these two converters (Eqs 4.7 and 4.8) that the crucial coupling between the pheromone molecule micro level and the walker ant macro level takes place. Kugler & Turvey (1987) and Parunak & Brueckner (2001) emphasize how crucial this coupling is for walkers, enabling them to find their target at the macro level by climbing the pheromone molecule grid at the micro level. Computing uncertainty about the pheromone molecules' location from Eq. 1 is equivalent to assessing micro-level agent state, while uncertainty about the walker ants' location defines macro-level agent state (Fig. 5 and Table 5).

Figure 5
The CASOS location uncertainty (U) sector

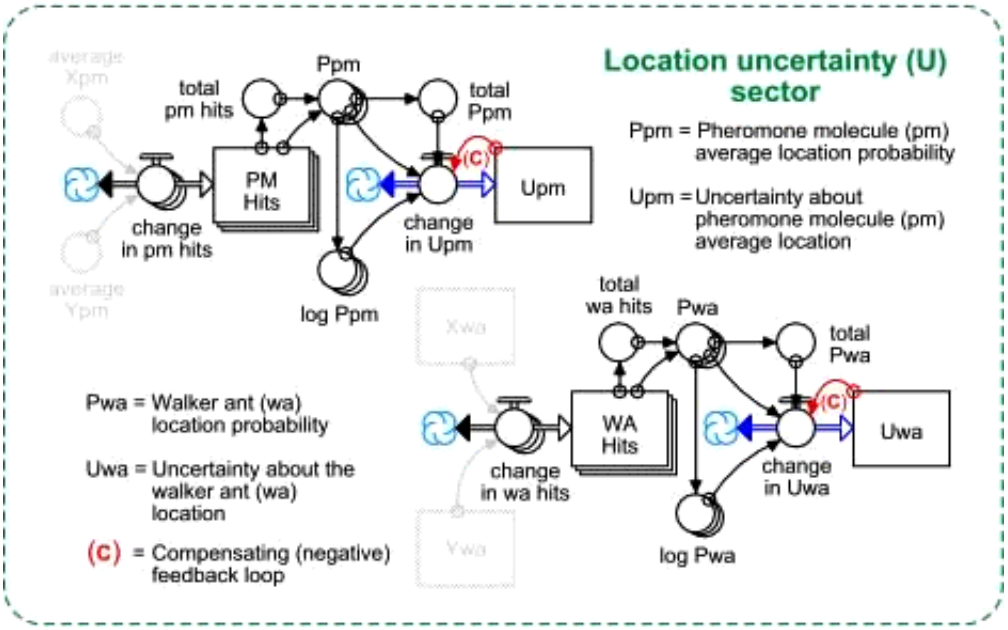


To make it so, Parunak & Brueckner (2001, Fig. 2, p. 127) suggest tiling the macro- and micro-level grids of Fig. 1 and then computing location probabilities by counting the pm and wa populations that hit each tile. Although Parunak & Brueckner measure entropy in terms of both location and direction, the CASOS location uncertainty (U) sector only computes uncertainty about agent location. Moreover, their 15×15 tiling would require a total of 225 array elements per dimension, but Table 5 gets away with only 16, thanks to a 4×4 tiling scheme.

Parunak & Brueckner (2001) choose their tiling scheme empirically by observing running simulations. Extreme cases, i.e. a 1×1 grid, notwithstanding, grid resolution has no effect on the shape of entropy/uncertainty increase, but simply reduces its time to saturation, i.e. U reaching its upper bound of one. Also, they compute location probabilities by averaging over multiple simulation runs, but this model computes agent location probabilities and uncertainty dynamically through time, within each Monte Carlo (3.14) simulation experiment.

Table 5 Location uncertainty (U) sector equations

| *Level or state variables (stocks)* | *Eq. #* |
|---|---|
| PM Hits[Tile # pm](t) = PM Hits[Tile # pm](t - dt) + (change in pm hits[Tile # pm]) * dt | (5.1) |
| INIT PM Hits[Tile # pm] = 0 {unit = hits} | (5.1.1) |
| Upm(t) = Upm(t - dt) + (change in Upm) * dt | (5.2) |
| INIT Upm = 0 | (5.2.1) |
| Uwa(t) = Uwa(t - dt) + (change in Uwa) * dt | (5.3) |
| INIT Uwa = 0 | (5.3.1) |
| WA Hits[Tile # wa](t) = WA Hits[Tile # wa](t - dt) + (change in wa hits[Tile # wa]) * dt | (5.4) |
| INIT WA Hits[Tile # wa] = 0 {unit = hits} | (5.4.1) |
| *Rate variables (flows)* | |
| change in pm hits[1] = IF (10 <= average Xpm AND (average Xpm < 25) AND (10 <= average Ypm) AND (average Ypm < 25)) THEN (1) Else (0) {unit = hits / t} | (5.5) |
| M | (5.M) |
| change in pm hits[16] = IF (55 <= average Xpm AND (average Xpm < 70) AND (55 <= average Ypm) AND (average Ypm < 70)) THEN (1) Else (0) {unit = hits / t} | (5.20) |
| change in Upm = (total Ppm - Upm) * ( - ((Ppm[1] * log Ppm[1] + Ppm[2] * log Ppm[2] + Ppm[3] * log Ppm[3] + Ppm[4] * log Ppm[4] + Ppm[5] * log Ppm[5] + Ppm[6] * log Ppm[6] + Ppm[7] * log Ppm[7] + Ppm[8] * log Ppm[8] + Ppm[9] * log Ppm[9] + Ppm[10] * log Ppm[10] + Ppm[11] * log Ppm[11] + Ppm[12] * log Ppm[12] + Ppm[13] * log Ppm[13] + Ppm[14] * log Ppm[14] + Ppm[15] * log Ppm[15] + Ppm[16] * log Ppm[16]) / LOG10(10))) | (5.21) |
| change in Uwa = (total Pwa - Uwa) * ( - ((Pwa[1] * log Pwa[1] + Pwa[2] * log Pwa[2] + Pwa[3] * log Pwa[3] + Pwa[4] * log Pwa[4] + Pwa[5] * log Pwa[5] + Pwa[6] * log Pwa[6] + Pwa[7] * log Pwa[7] + Pwa[8] * log Pwa[8] + Pwa[9] * log Pwa[9] + Pwa[10] * log Pwa[10] + Pwa[11] * log Pwa[11] + Pwa[12] * log Pwa[12] + Pwa[13] * log Pwa[13] + Pwa[14] * log Pwa[14] + Pwa[15] * log Pwa[15] + Pwa[16] * log Pwa[16]) / LOG10(10))) | (5.22) |
| change in wa hits[1] = IF (10 <= Xwa AND (Xwa < 25) AND (10 <= Ywa) AND (Ywa < 25)) THEN (1) Else (0) {unit = hits / t} | (5.23) |
| M | (5.M) |
| change in wa hits[16] = IF (55 <= Xwa AND (Xwa < 70) AND (55 <= Ywa) AND (Ywa < 70)) THEN (1) Else (0) {unit = hits / t} | (5.38) |
| *Auxiliary variables and constants (converters)* | |
| log Ppm[1] = IF (Ppm[1] = 0) THEN (0) ELSE (LOG10(Ppm[1])) | (5.39) |
| M | (5.M) |
| log Ppm[16] = IF (Ppm[16] = 0) THEN (0) ELSE (LOG10(Ppm[16])) | (5.54) |
| log Pwa[1] = IF (Pwa[1] = 0) THEN (0) ELSE (LOG10(Pwa[1])) | (5.55) |
| M | (5.M) |
| log Pwa[16] = IF (Pwa[16] = 0) THEN (0) ELSE (LOG10(Pwa[16])) | (5.70) |
| Ppm[1] = PM Hits[1] / total PM hits | (5.71) |
| M | (5.M) |
| Ppm[16] = PM Hits[16] / total PM hits | (5.86) |
| Pwa[1] = WA Hits[1] / total WA hits | (5.87) |
| M | (5.M) |
| Pwa[16] = WA Hits[16] / total WA hits | (5.102) |
| total pm hits = ARRAYSUM (PM Hits[*]) + 1 {unit = hits} | (5.103) |
| total Ppm = ARRAYSUM(Ppm[*]) | (5.104) |
| total Pwa = ARRAYSUM(Pwa[*]) | (5.105) |
| total wa hits = ARRAYSUM (WA Hits[*]) + 1 {unit = hits} | (5.106) |

Initialized at zero (Eqs 5.1.1 and 5.4.1), the one-dimensional arrayed PM Hits[·] (5.1) and WA Hits[·] (5.4) stocks count the total number of times the average pm and wa agents hit each tile of their superimposed 4×4 tiling schemes, respectively. Each time the average pheromone molecule hits the first pm tile [Tile # pm = 1], for example, the change in pm hits[1] flow array

(5.5) adds a hit to the PM Hits[1] stock array (5.1). Similarly, each time a wa agent hits the 15th walker ant tile [Tile # wa = 15], the change in wa hits[15] flow array (5.37) adds a hit to the WA Hits[15] stock array (5.4).

Subsequently, the Ppm[1] converter array (5.71) computes the probability of the average pm hitting the first pm tile [Tile # pm = 1] as the ratio of the PM Hits[1] stock array over the total pm hits array sum (5.103). Similarly, the Pwa[15] converter array (5.101) computes the probability of the wa hitting the 15th wa tile [Tile # wa = 15] as the ratio of the PM Hits[1] stock array over the total pm hits array sum (5.103). Adding a hit to these array sum converters (Eqs 5.103 and 5.106) prevents their dividing by zero when all tiles are empty.

Once the arrayed Ppm[·] (Eqs 5.71–5.86) and Pwa[·] (Eqs 5.87-5.102) converters compute the micro- and macro-level agent location probabilities, respectively, the log Ppm[·] (Eqs 5.39–5.54) and log Pwa[·] (Eqs 5.55-5.70) calculate their respective logarithms. Together, the probabilities, their logarithms and the total probability array sums (5.104 and 5.105) affect the change in Upm (5.21) and change in Uwa (5.22) flows that feed their respective pm and wa agent location uncertainty stocks Upm (5.2) and Uwa (5.3). Each of the change in Upm (5.21) and change in Uwa (5.22) flows use Shannon's uncertainty formula (Eq. 1).

In the case of micro-level uncertainty about the pm average location (Upm), Shannon's positive constant *k* gets smaller as Upm increases and its difference from the total pheromone molecule average location probability (5.104) decreases. Similarly, in the case of macro-level uncertainty about the walker ant location (Uwa), Shannon's positive constant *k* gets smaller as Uwa increases and its difference from the total wa location probability (5.105) declines. In both cases (5.21 and 5.22), following Parunak & Brueckner's (2001) suggestion, dividing the reported agent location uncertainties by log(10) makes the logarithms' base irrelevant.

One might as well call Fig. 6 and Table 6 the *George P. Richardson sector*. Richardson's (1995) contribution helps detect shifting feedback loop polarity and loop dominance in system dynamics models. The ant pheromone-driven CASOS contains multiple feedback loops clearly marked as compensating (C) or reinforcing (R) on Fig. 3 through Fig. 5. Both the pm micro level (Fig. 3) and the location uncertainty (Fig. 5) sectors show straightforward compensating or negative (balancing) loops. The walker ant macro level (Fig. 4), however, contains four nested bipolar loops, which make Richardson's rigorous approach most relevant to their assessment.

Treating the Ywa dimension of the walker ant's location as a constant parameter (6.1) allows a *ceteris paribus* investigation of the feedback loops that implicate the Xwa dimension of walker location. Similarly, smoothing the biased Xwa change (6.2) flow and Xwa (6.3) stock over a long period of 50 time (t) units weeds out random variation in the walker ant sector.

Equations 6.4 through 6.6 implement Richardson's (1995) approach to detecting shifting loop polarity (slp) in nonlinear first-order feedback systems of the form $dx/dt = x\ f(x)$. He suggests constructing the $f(\text{Xwa})$ function (6.4) and $f(\text{Xwa}) / \text{Xwa}$ ratio (6.5), and computing the negative derivative of the $f(\text{Xwa})$ function with respect to Xwa (6.6). Although the number one parameter (6.4 and 2nd line of Eq. 6.6) does not affect the computation, it is a reminder that the walker ant step (4.12) is a component of the $f(\text{Xwa})$ function.

A structural change helps resolve the macro level's slp. The target ant coordinates Xta and Yta, shown as ghosts on Fig. 4, replace the average Xpm and average Ypm converters in Eqs 6.4 and 6.6. This change is precisely where the CASOS' macro level is coupled crucially to its micro level but, as the beyond entropy: feedback-loop structure section shows, tampering with model structure is worth it when one seeks to expose slp rigorously in nested bipolar loops.

Figure 6
The shifting loop polarity (slp) detection sector

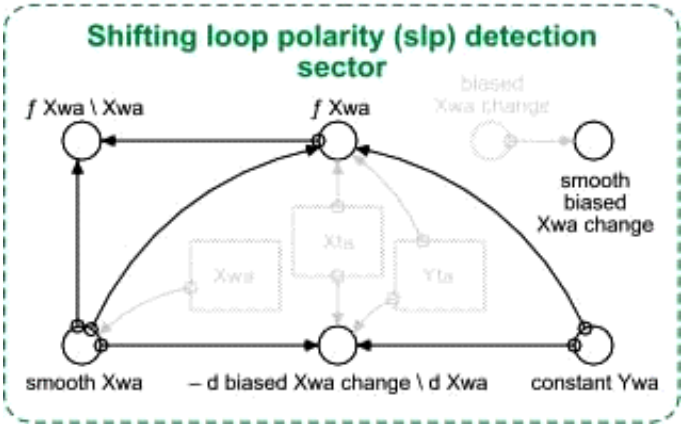


Table 6 Shifting loop polarity (slp) detection sector equations

| Auxiliary variables and constants (converters) | |
|---|---|
| constant Ywa = 44 {unit = step} | (6.1) |
| smooth biased Xwa change = SMTH3 (biased Xwa change, 50) {unit = step/t} | (6.2) |
| smooth Xwa = SMTH3 (Xwa, 50) {unit = step} | (6.3) |
| ƒ Xwa = ((Xta - smooth Xwa) / (SQRT ((Xta - smooth Xwa)^2) + ((Yta - constant Ywa) ^2))) * 1 | (6.4) |
| ƒ Xwa \ Xwa = ƒ Xwa / smooth Xwa | (6.5) |
| – d biased Xwa change \ d Xwa = -(-1 / (((Xta - smooth Xwa)^2) + (((Yta - constant Ywa)^2)^(1/2)))) -((1 * (Xta - smooth Xwa) * (2 * smooth Xwa - 2 * Xta)) / ((((Xta - smooth Xwa)^2) +((Yta - constant Ywa)^2)^(1/2))^2)) | (6.6) |

## Experimental results

The results reported here entail setting *iThink Analyst's* (Richmond et al. 2000) run specs as follows: simulation length TIME ∈ [0, 250], with a computation interval dt = 1 and Euler's integration method. These settings match Parunak & Brueckner's (2001) specifications.

The arrows on the phase plot of Fig. 7 (top panel) show how the pheromone molecules' average location changes through time. While stationary, the target ant (ta) deposits one molecule at location (50, 50) every time step. As the pheromone molecules diffuse through the environment, they create a gradient the walker ant (wa) can follow.

Although the two agents desire to be together, neither knows the location of the other. The walker ant (wa) wants to reach its (50, 50) destination, but is uncertain about where to go. The lower panel of Fig. 7 shows the pm average location probability (Ppm) after 30 simulation runs. Although pheromone molecules diffuse through the environment and evaporate, the surface plot of Fig. 7 (cut out to add drama) shows that the walker has a fair chance to find its target ant (ta).

The phase plot of Fig. 8 shows an ensemble of 30 wa agents with perceptual radius r = 25 (4.11). These walkers follow the pm micro grid of pheromone molecules (Fig. 7) that the target emits. Just like in Parunak & Brueckner's (2001, Fig. 5, 7 and 8, p. 128) experimental results, this model's walker ants also follow three distinct path groups:

**I.** Initially (lower left, phase plot of Fig. 8), each wa wanders randomly around its (30, 30) origin until the average pm wavefront, diffusing and evaporating from (50, 50), enters its perceptual radius $\rho$. In this Brownian motion region, walkers have no guidance because ta's pheromone molecules are invisible to them.

**II.** When walkers sense the pm average inside their $\rho$, then they move swiftly from their initial (30, 30) region toward ta's (50, 50) region (middle, phase plot of Fig. 8). They can now sense ta and follow the pm average grid under Brownian motion.

**III.** When they reach ta's (50, 50) region (upper right, phase plot of Fig. 8), walkers seem to meander again as if performing a random walk. The truth is, however, that walkers now deterministically follow ta's pheromone molecules, which are executing a random walk under Brownian motion. This is where this model differs from Parunak & Brueckner's (2001) brilliant multi-agent CASOS study.

Figure 7
Pheromone molecule (pm) average location and location probability (Ppm)

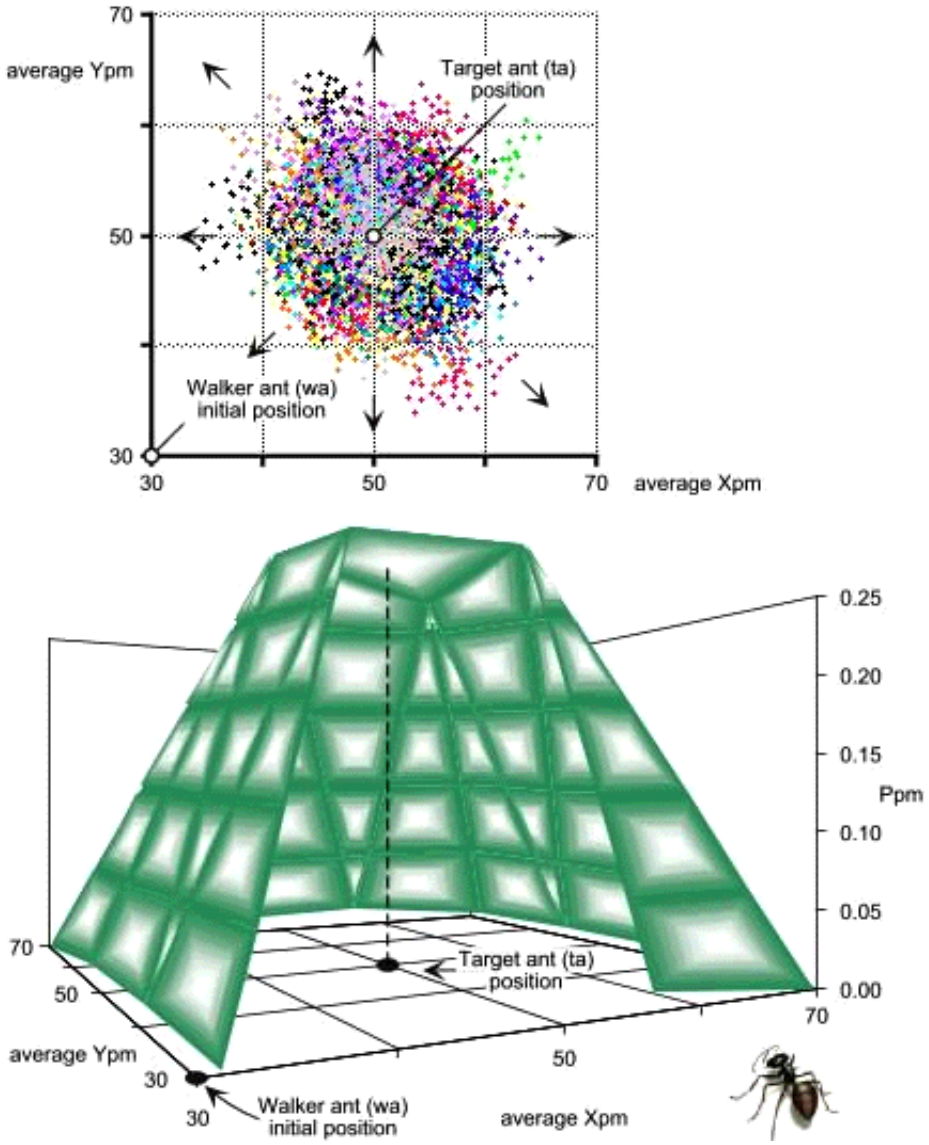


The 3D column chart of Fig. 8 shows how the walker ants' location probability (Pwa) values are distributed over the macro-level 4×4 grid, after 30 simulation runs. Subsequently, these Pwa values determine the CASOS' macro-level location uncertainty (Uwa), while the Ppm values determine the average pm micro-level location uncertainty (Upm) through time (Fig. 9a).

Figure 8
Ensemble of guided walker ant (wa) paths and location probability (Pwa)

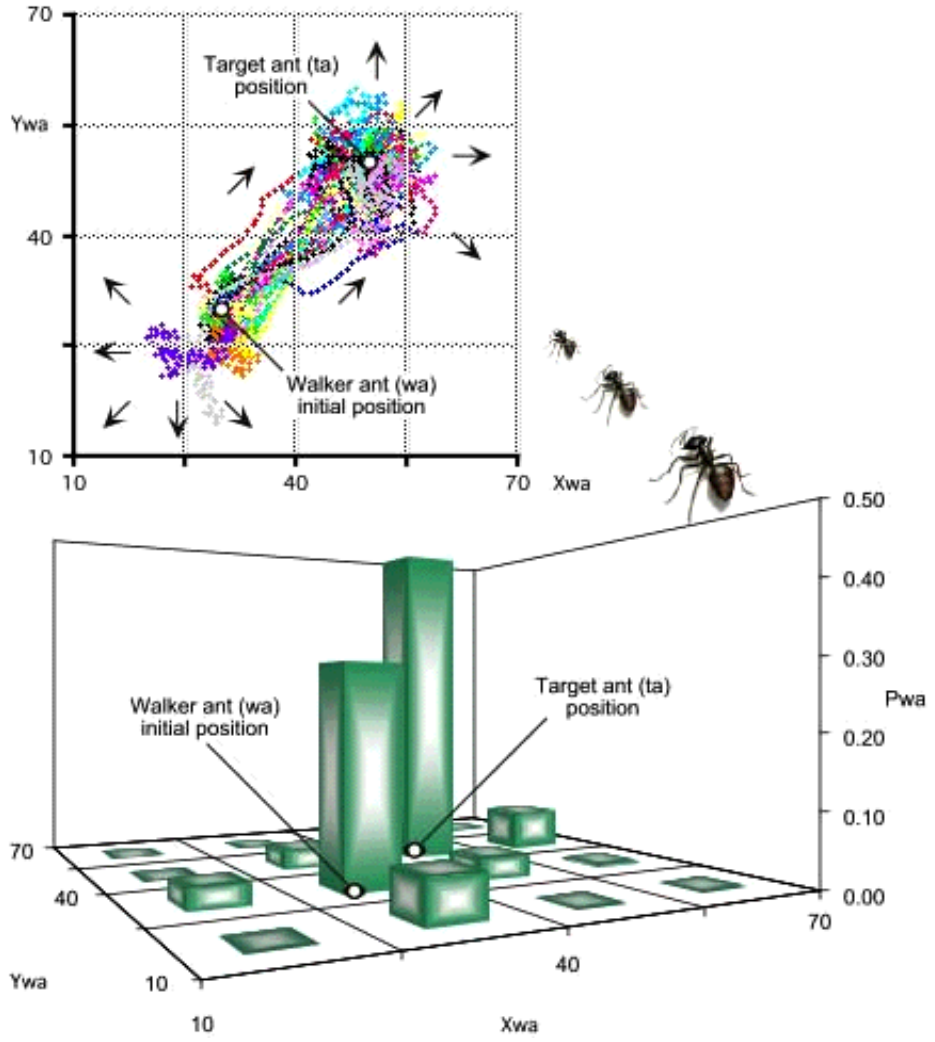


Very similar to Parunak & Brueckner's (2001, Fig. 4, p. 127) micro-level entropy results, the typical uncertainty about the pm average location (Upm) on Fig. 9a increases through time until it saturates at one. The more pheromone molecules enter the system and disperse throughout their 4×4 pm grid (Fig. 1 and 7), the higher Upm grows.

Similarly, the typical walker initially wanders randomly around its origin. Unguided, as if uncoupled from the pheromone molecule micro-level, its behavior is identical to that of the typical average pm. Consequently, Uwa is initially identical to Upm (Fig. 9a). Once wa senses the pm average inside its perceptual radius r, however, then if follows it rather directly, now guided by the pm grid its target creates. Although the guided macro-level Uwa continues to rise, it does so at a lower rate than when wa is unguided (Fig. 9a). There is less uncertainty at the macro level about wa's whereabouts when guided by the micro-level pm grid ta creates.

But when it reaches ta's region, the walker seems to meander again as if performing a random walk because ta's pm average executes its random Brownian motion CONTINUOUSLY throughout each simulation run. Faithfully following the pheromone molecules' random walk, the walker emulates their random behavior. Consequently, like Upm, Uwa also rises rapidly and *concomitantly*, just as Kugler & Turvey (1987) predict, until it too saturates at its maximum

value of one. With wa still guided, the macro-level uncertainty about its whereabouts now matches the uncertainty about the pheromone molecules' average location, i.e., Uwa = Upm = 1.

Figure 9
Uncertainty (U) about location in the CASOS micro and macro levels

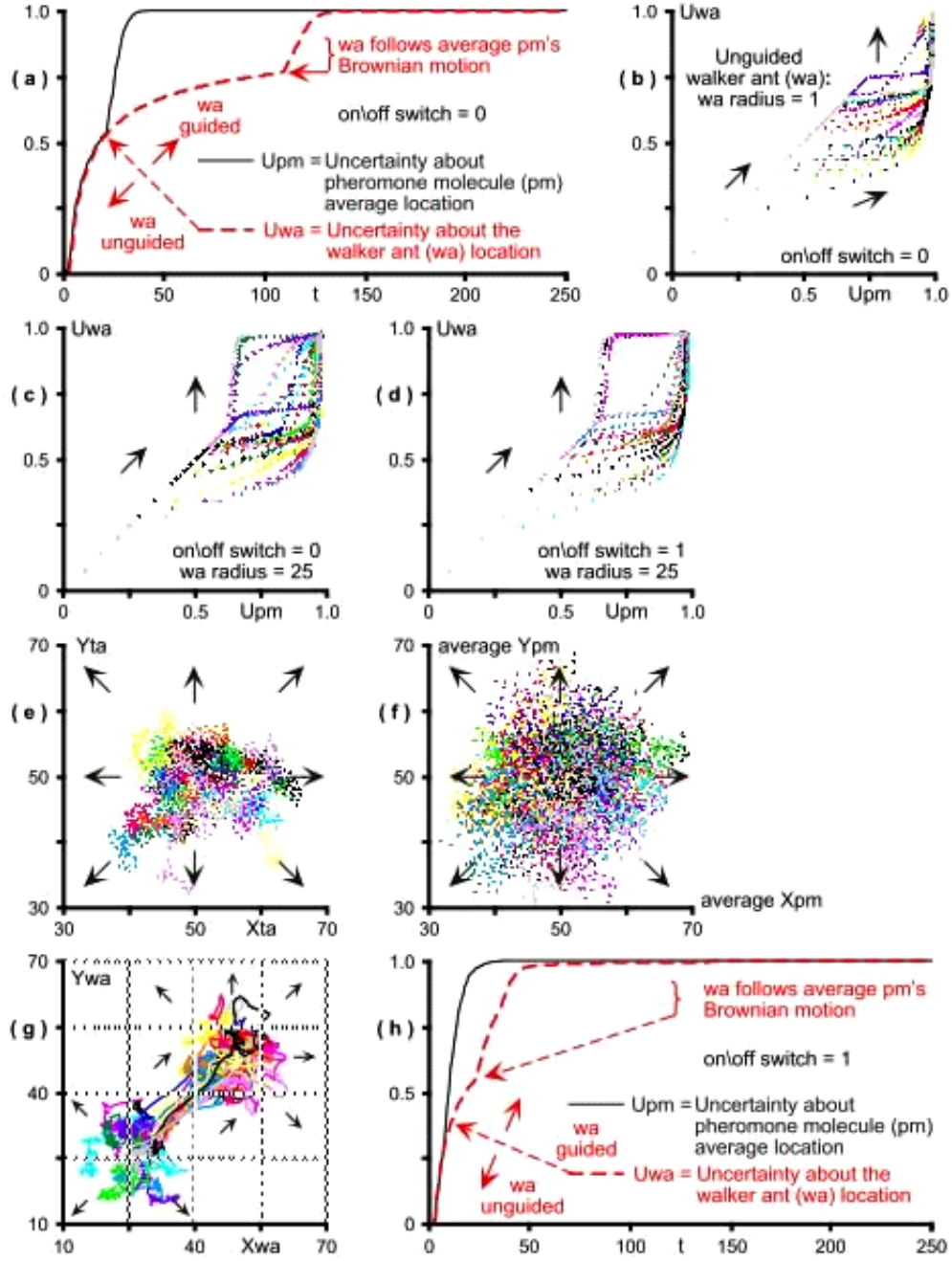


The phase plot of Fig. 9b shows how Upm and Uwa relate to each other when walker ants stay unguided longer because of a small perceptual radius, $\rho$ = 1. While ta remains stationary, i.e., on\off switch = 0 (2.5), Uwa can stay concomitant to Upm longer because the average pm takes a long time to reach each walker's now tiny perceptual radius. Even then, however, Uwa stays rather consistently less than or equal to Upm because their small $\rho$ makes it virtually impossible for walkers to make an early run for ta's location.

With $\rho$ reset to 25 (Fig. 9c), some walkers sometimes perceive their target early, before pheromone molecules have a chance to diffuse far enough from ta's initial location. When that happens, the average pm location guides walkers early and Uwa exceeds Upm for a while. Eventually, however, whether early or late, walkers always fall pray to the average pheromone's Brownian motion and the inevitable happens: Uwa = Upm = 1. Both the macro and the micro CASOS levels become equally uncertain about their respective agents' location. Interestingly enough, when the stationary ta turns mobile, i.e. on\off switch = 1, then Uwa exceeds Upm less (Fig. 9d). Doubling randomness at the micro level causes Upm to seclude Uwa more frequently, thereby sequestering the agent location uncertainty Uwa at the macro level.

As target ants now meander continuously under their newly acquired mobility (Fig. 9e), they cause the pheromone molecules they emit to diffuse more vigorously through the environment (compare Fig. 9f to the phase plot of Fig. 7). Because of their initial random walk around their origin, walkers in different runs again will be at different locations when they start to sense a ta and will follow slightly different paths to their target (Fig. 9g). The excess pm randomness at the micro level, however, while still sequestering uncertainty/entropy at the macro level, it does so for a shorter time. It shortens both the time a typical wa stays unguided and the time it takes a walker to move to the now enlarged ta region (Fig. 9h; compare to Fig. 9a).

In addition to confirming Kugler & Turvey's (1987) concomitant entropy prediction as well as some of Parunak & Brueckner's (2201) dynamics, these results are consistent with the self-organization seen in cybernetics, dissipative structures and thermodynamic fluctuations, where the larger their randomness, the faster systems become autopoietic, i.e., produce order. While Upm sequesters Uwa in most cases, the larger the uncertainty about the pheromone molecules' average location at the micro level, the faster the macro system self-organizes, i.e. the faster walkers move from their initial region to their now mobile target's region. Doubling randomness at the micro level pushes the system as a whole faster to its stable point attractor, where Uwa = Upm = 1.

Where these results differ, however, from Parunak & Brueckner's (2001, Fig. 6, p. 128), is in the unguided walker entropy (here Uwa). How is it possible for the unguided walker, when it acts just like a pm, executing a random walk, to produce entropy so vastly different from the pheromones'? The vast discrepancy between their Fig. 4 (p. 127) and Fig. 6 (p. 128) makes one wander about their method. This essay's Fig. 9 shows that, even under different experimental conditions, Upm and Uwa are identical as long as the pheromone molecules at the micro level and the unguided walker ants at the macro level are executing random walks. Moreover, while trying to assess entropy in the overall CASOS, Parunak & Brueckner finally ask whether sequestering "macro (walker) entropy is causally related to the increase in micro entropy, or just coincidental" (2001, p. 129). Even if rhetorical, this question begs for a system dynamics demonstration. How well can system dynamics explain causal relations in circular feedback loops that produce nonlinear dynamics spontaneously out of their local interactions? Let's see.

**Beyond entropy: feedback-loop structure**

Figures 10 though 14 revisit the model's sectors. Phase plots highlight causal relations among variables embedded in feedback loops and confirm loop polarity. Within each sector, the X and Y location dimensions are embedded in symmetrical loops, so Fig. 10 though 14 show relations that involve the X dimension only.

The pheromone molecule (pm) sector (Fig. 3) contains three compensating (negative) feedback loops, their negative links so marked on Fig 10 because they emanate from outflows. This is an influence diagramming (ID) convention that system dynamicists accept even when

they define loop polarity rigorously (Richardson 1995). But these loops' real polarity depends on time to evaporate (3.17), a random parameter whose sign is set by environmental conditions outside the loops. Although the nonlinear negative relation between time to evaporate (3.17) and the pm evaporation (3.5) outflow (Fig. 10a) plays outside these loops, it does turn them positive. Then, they drive the pm average so far that walkers never sense their targets. Or, alternatively, they bring it inside the wa's perceptual radius so fast that uncertainty about walker location at the macro level (Uwa) exceeds Upm at the micro level (Fig. 9c and d).

Figure 10
The pheromone molecule (pm) sector (micro level) feedback loops with phase plots

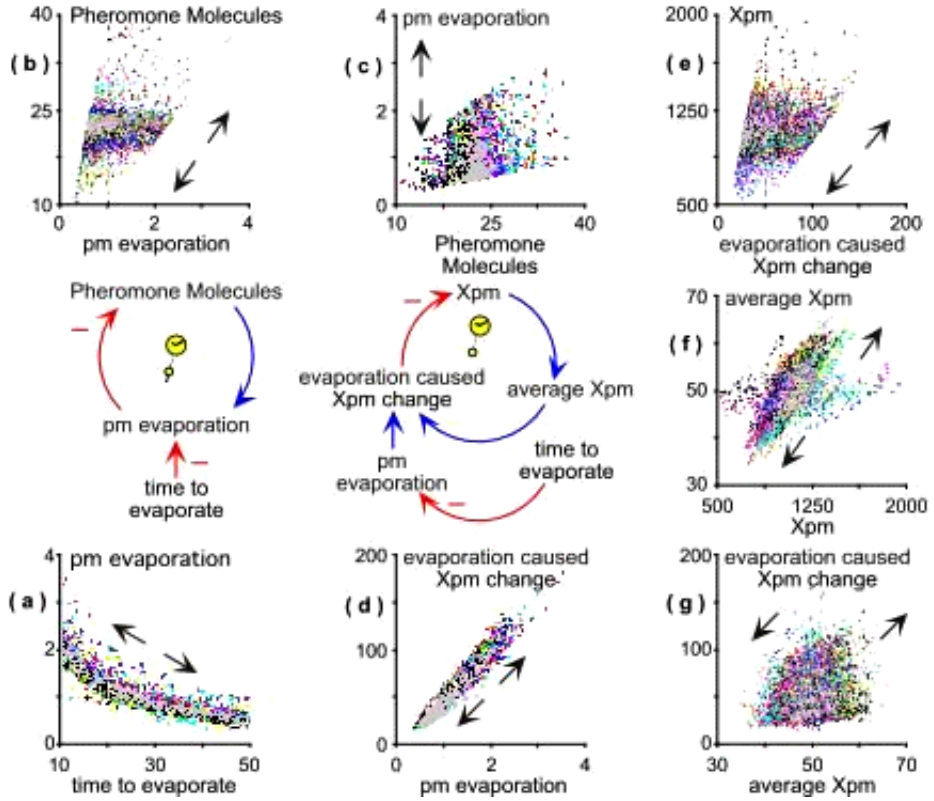


The walker ant (wa) sector of Fig. 4 contains six nested feedback loops. Three of them affect wa's X location dimension and three its Y dimension. Four of the loops are bipolar, marked as (C)/(R) on Fig. 4. Figures 11 through 13 show the X dimension loops in detail.

The macro-level bipolar loop that involves random Xwa change (4.3) shows some interesting relations among its variables (Fig. 11) because of the randomness this loop handles. The distance formula in 4.9 explains the bipolar relation between difference in X (4.7) and distance (4.9). Worth noting is how the relations between distance and random Xwa change (Fig. 11c) and between the random Xwa change flow and the Xwa (4.1) stock (Fig. 11d) confirm the orthogonality between wa's biased and random motion components. Both phase plots show that this model behaves consistently with Parunak & Brueckner's (2001, p. 126) $\vec{G} + \vec{R}$ vector sum, where $\vec{G}$ is equivalent to wa's guided motion and $\vec{R}$ corresponds to its random walk.

The feedback loop of Fig. 11 is active only when pheromone molecules are outside the walker's radius $\rho$. Then wa cannon perceive ta and walks randomly, just like a pm. This loop also explains the behavior of walkers who never meet their target. When all links of Fig. 11 turn positive, then its loop becomes a reinforcing one, sometimes sending wa to meander so far that

the pm average cannot ever enter its perceptual radius. Oddly enough, the same loop can also explain the behavior of walkers who go meet their target so fast that uncertainty about walker location at the macro level (Uwa) exceeds Upm at the micro level (Fig. 9c and d).

Figure 11
The walker ant (wa) sector (macro level) random Xwa change bipolar feedback loop with phase plots

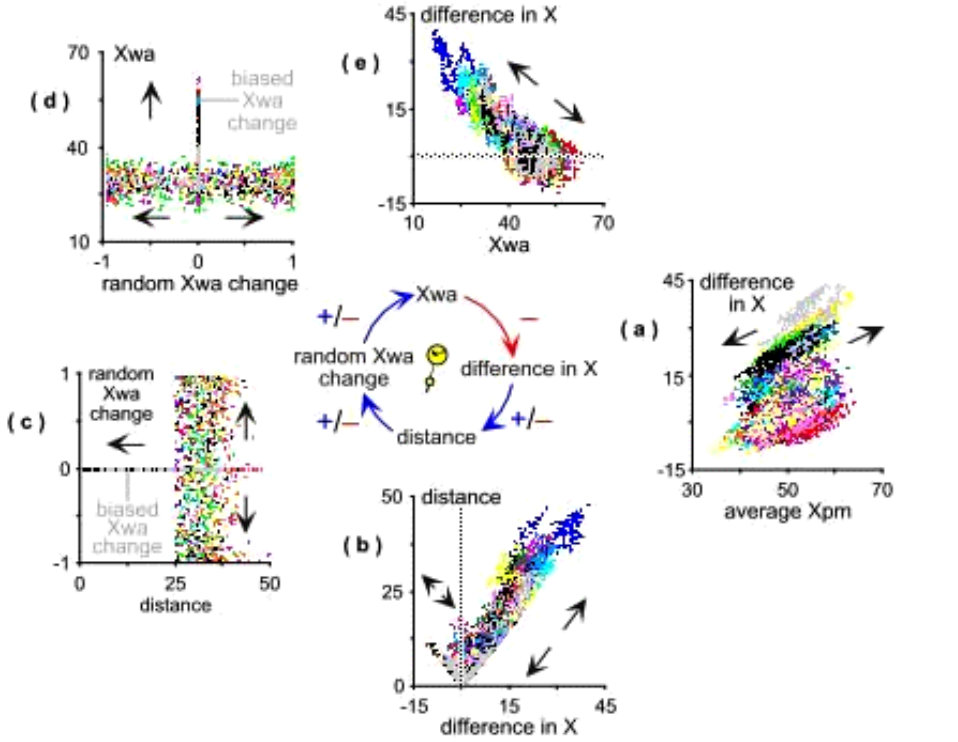


The wa sector's (Fig. 4) unipolar (R) loops look innocent. One positive relation (Fig. 12a) and two negative ones (Fig. 12b and 12c) make up a straightforward reinforcing or positive feedback loop. Right?

Wrong! Figure 12 is a perfect example of what made Richmond (1980) define a positive loop as a goal-seeking loop whose goal continuously runs off in the direction of the search. In response, Richardson (1995) explains that the negative polarity always dominates positive loops with gain less than one. Not only does the biased Xwa change (4.4) flow always fluctuate between ±1 (Fig. 12a and b), but even difference in X (4.7) sometimes falls inside the ±1 zone (Fig. 12c). Despite its unipolar (R) sign on Fig. 4, the loop's polarity depends on difference in X (4.7). At least the loop reconfirms once more the orthogonality between the biased ($\dot{G}$) and the random ($\dot{R}$) components of wa's motion (Fig. 12b). And so do the relations of Fig. 13c and d.

Together, the nested feedback loops of Fig. 12 and 13 determine wa's behavior when it senses ta though the continuously random-walking pm grid the latter creates. And much like its random counterpart (Fig. 11), the biased component loop of wa's motion (Fig. 13) can also turn positive. That is how it biases, i.e. reinforces, walkers to go meet their target fast. So fast, in fact, that pheromone molecules cannot diffuse far enough from ta's initial location for Upm to sequester Uwa (Fig. 9c and d). The loop causes wa to respond to pm's average location through the average Xpm (3.12) effect on the difference in X (Fig. 13a). Together, the difference in X (4.7) and difference in Y (4.8) determine distance (4.9), which always returns a nonnegative number

(Fig. 13b). The net effect of distance on Xwa (4.1) is negative relation (Fig. 13e) and, closing the circle, Xwa (4.1) has a negative effect on the difference in X (Fig. 13f).

Figure 12
The walker ant (wa) sector biased Xwa change reinforcing feedback loop with phase plots

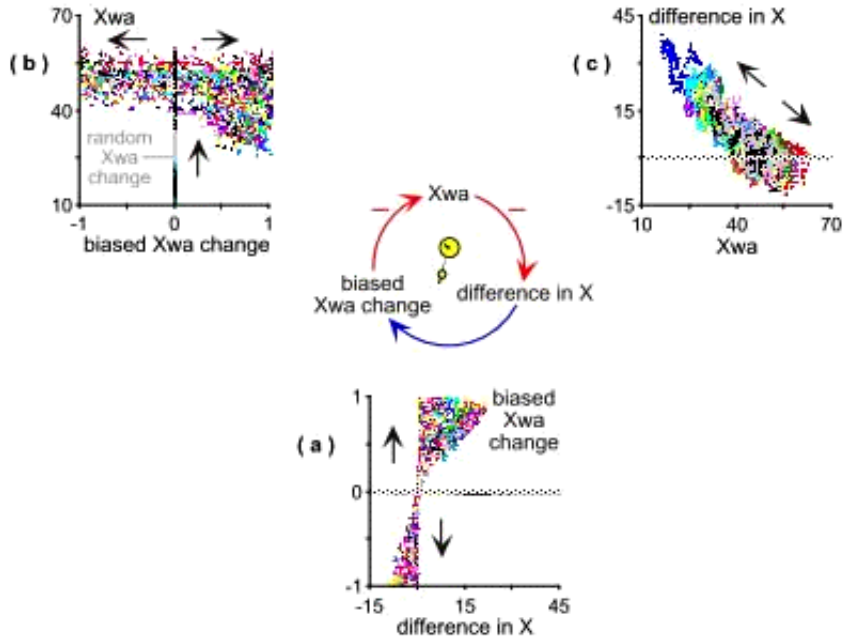


Corresponding to the (C) loops of Fig. 5, the right panel of Fig. 14 confirms the negative effects of Upm (5.2) and Uwa (5.3) on their respective change in Upm (5.21) and change in Uwa (5.22) inflows. The top left panel of Fig. 14 shows how uncertainty about pm average location at the micro level (Upm) responds to the random Xpm change (3.7) flow that keeps pheromone molecules under Brownian motion continuously. Saturation is clear at Upm = 1.

Similarly, the lower left panel of Fig. 14 shows how uncertainty about walker location at the macro level (Uwa) relates causally to the smooth biased Xwa change (6.2) flow that moves wa when it responds deterministically to the pheromone molecules' random walk. The phase plot's time-direction arrows mark two distinct dynamics. One renders the relation between wa's biased motion and Uwa first positive and then orthogonal, after Uwa reaches its Uwa = 1 point attractor. The other shows the same relation to be first positive, then to turn negative and, just as Uwa again saturates at its stable point attractor Uwa = 1, to become orthogonal once more.

The capricious relation between the walker's biased motion and macro-level uncertainty about its whereabouts prompts a more in-depth analysis that splits wa's biased motion into two. *First*, one must look for shifting loop polarity (slp) during walkers' transition between their distinct path groups **I** and **II**. *Second*, to reassess slp during the transition between distinct path groups **II** and **III**. In both cases, Richardson (1995) helps examine slp rigorously (Fig. 15).

The phase plot of Fig. 15 shows the $f$(Xwa) function (6.4), $f$(Xwa) / Xwa ratio (6.5) and negative derivative of $f$(Xwa) with respect to Xwa (6.6), smoothed over 50 time (t) units to weed out random variation. The graph shows the last two quantities vertically magnified ten times. The negative derivative of $f$(Xwa) with respect to Xwa represents the negative slope of the tangent to the graph of $f$(Xwa) at the point (Xwa, $f$(Xwa)). The $f$(Xwa) / Xwa ratio is the slope of the line from the graph's origin to the same point (Xwa, $f$(Xwa)). Together, these two lines form the di-

agonals of a rectangle with sides parallel to the horizontal and vertical axes. Where the two lines meet is where the $Xwa_o$ point lives; where loop polarity shifts.

Figure 13
The walker ant (wa) sector biased Xwa change bipolar feedback loop with phase plots

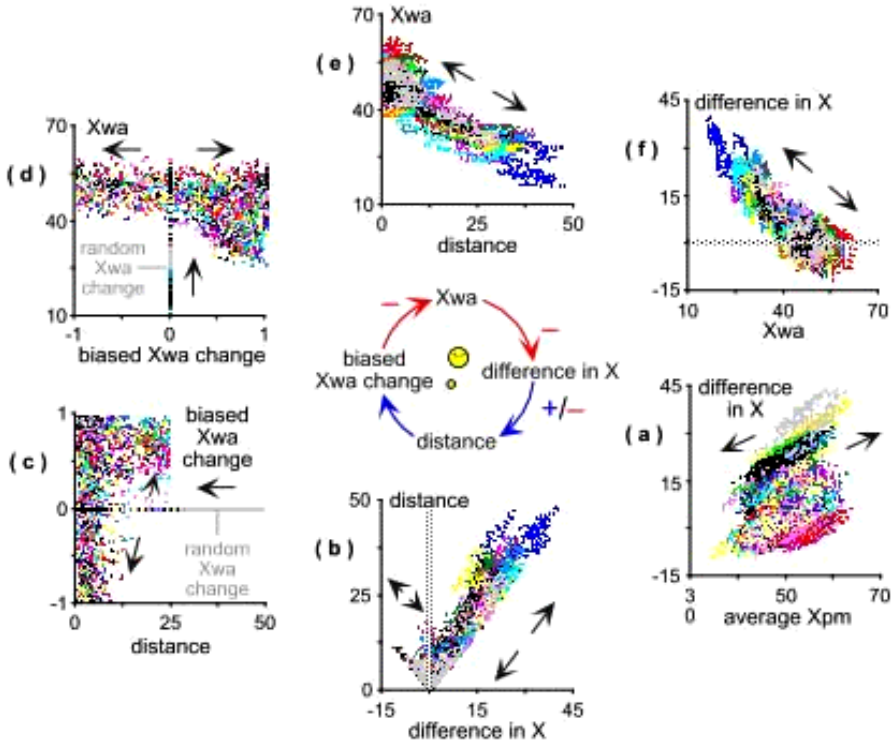


Figure 14
The CASOS location uncertainty (U) sector feedback loops with phase plots

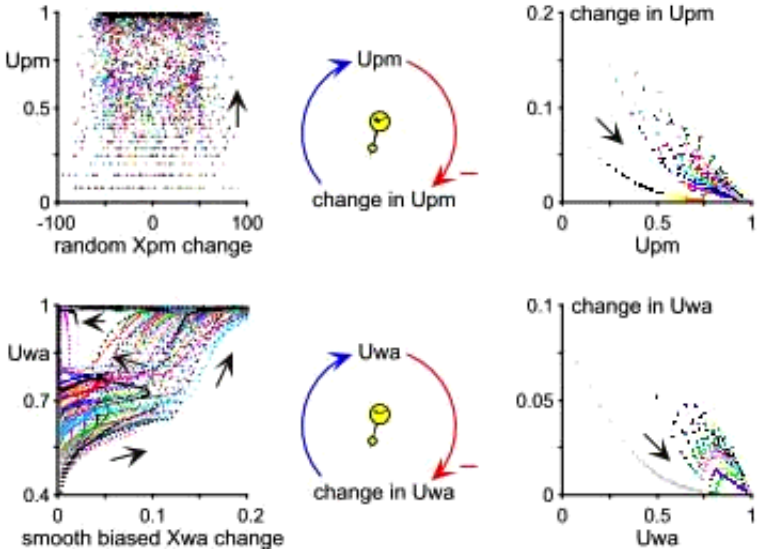


Treating wa's Ywa location dimension as if it were constant (6.1), yields a *ceteris paribus* examination of the nested feedback loops that implicate wa's Xwa location dimension (Fig. 11, 12 and 13). To isolate macro level slp during wa's transition along its distinct path groups **I** and **II**, ta's Xta and Yta coordinates replace the average Xpm and average Ypm converters in Eqs 6.4

and 6.6. This way, once walkers sense their target through its pheromones, they abandon random motion and head directly to ta's location as opposed to following the pm grid. Because of their initial random walk around their origin, walkers in different runs are at different locations when they sense ta and follow slightly different paths that converge to its location (Fig. 16a).

The five simulation runs of Fig. 16b entail replacing the Monte Carlo dummy (3.14) with the constant parameter Ywa (6.1). The resulting phase plot shows a range of $Xwa_o$ points where loop polarity shifts in the system.

Figure 15
Shifting loop polarity (slp) in the pheromone-driven CASOS

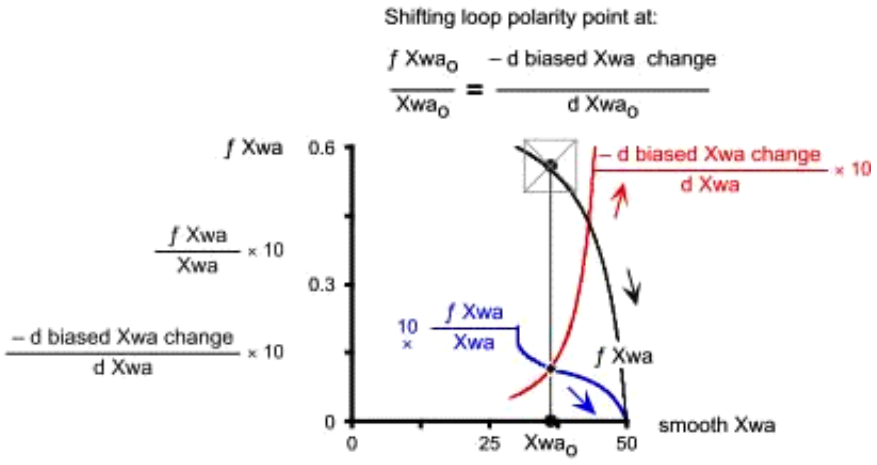


The actual dynamics of the typical walker's biased motion turns wa's (30, 30) origin into an unstable equilibrium point outside its random motion region. Positive (reinforcing) feedback dominates the system in the region where biased Xwa change has a positive slope. Negative (compensating) feedback is dominant where biased Xwa change has a negative slope (Fig. 16c). Once outside the random motion region, wa's biased motion rate initially rises nearly linearly and then, while still below $Xwa_o$, the system's behavior resembles pure exponential growth. As walkers approach ta's location, their biased motion continues to rise, but at a declining rate.

At $Xwa_o$, the biased Xwa change rate reaches a maximum. The peak of wa's biased motion curve corresponds to the inflection point on the trajectory of Xwa, i.e. the point at which the smooth Xwa stock is rising at its maximum rate. Beyond the inflection point of Fig. 16c, wa's biased motion, while still positive, drops, falling to zero just when the walker reaches the target ant's (50, 50) location, the system's new stable equilibrium point.

Inside walkers' random motion region or path group **I**, uncertainty about their location rises orthogonally to their smooth biased Xwa change rate (Fig. 16d). The phase plot shows how walkers' initial random motion accounts for at least 50 percent of location uncertainty at the macro level, i.e. Uwa = 0.5. Once the micro-level pheromones cause walkers' biased motion at the macro level, Uwa abandons its vertical climb and begins to rise concomitantly with the walkers' smooth biased Xwa change. As walkers move toward ta's location, the difference in X over the difference ratio inside the biased Xwa change (4.4) flow first rises nearly linearly, causing Uwa to rise at a declining rate. But once the walkers' biased motion rate begins to resemble pure exponential growth below $Xwa_o$ (Fig. 16c), Uwa also begins to rise faster again. By now walkers are far inside their path group **II**, so uncertainty about their location rises fast.

Then, just before it reaches its maximum, biased Xwa change begins to rise at a declining rate. Uwa again matches the biased motion's declining rise until it saturates at Uwa = 1. By now,

biased Xwa change has reached its maximum and starts to decline toward zero as both Fig. 16c and the topmost time arrow on the phase plot of Fig. 16d show. When inside walkers' perceptual radius, the micro-level pheromones reveal ta's existence and cause macro level agents to move orderly toward its location. This orderly, autopoietic behavior the pheromones trigger is what sequesters Uwa at the system's macro level.

Figure 16
Shifting loop polarity (slp) along walker path groups I and II ($\rho$ = 25)

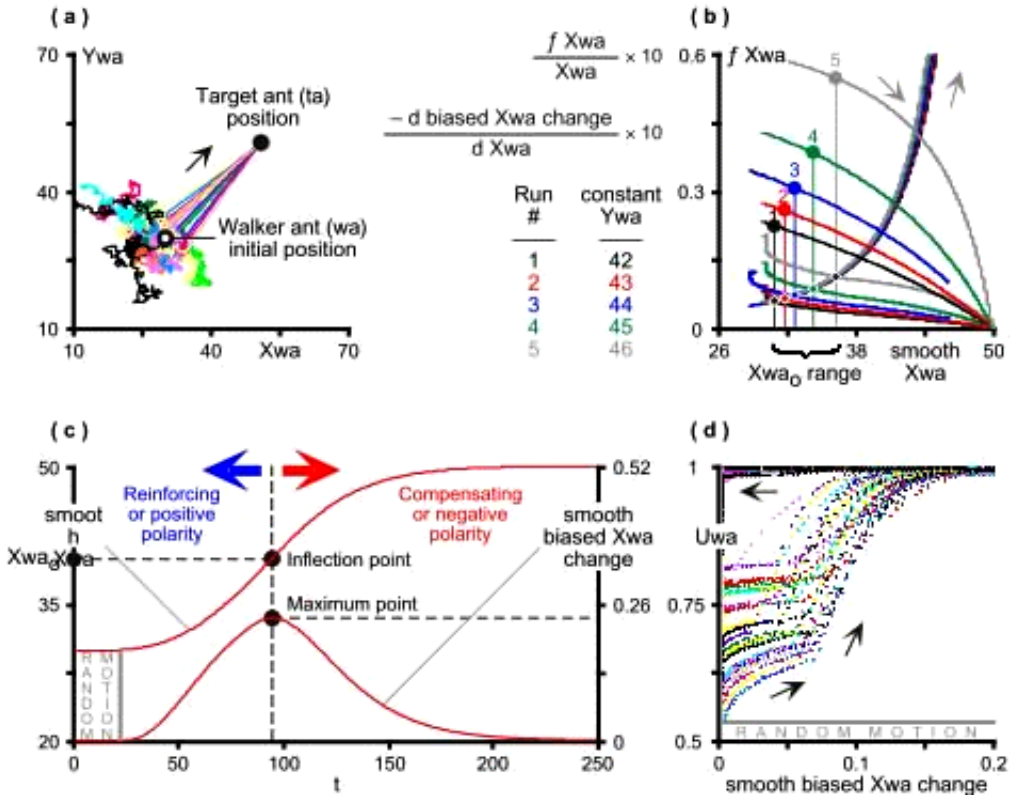


To reassess slp along path groups **II** and **III**, the average Xpm and average Ypm converters must be restored in Eqs 6.4 and 6.6, and the walkers' perceptual radius must increase drastically, i.e. $p$ = 50. Now walkers sense the target through the pm grid it creates at the outset, before they have a chance to meander under their own Brownian motion. But, as opposed to heading directly to their target's location, they follow the pheromone molecules' random motion deterministically, thereby departing from Parunak & Brueckner's quest for realism. Although walkers in different runs are at the same initial location when they sense ta, they follow divergent paths because of the pheromones' continuous random walk around ta's location (Fig. 17a).

The five runs of Fig. 17b again show that loop polarity shifts over the Xwa$_o$ range. The typical walker now leaves its initial (30, 30) location to go where it perceives its stationary target to be from the pm grid the target creates. Negative (compensating) feedback dominates as the negative slope of wa's biased Xwa change shows in the time domain of Fig. 17c. Initially, the walker's biased motion rate drops nearly linearly and the Xwa stock begins to grow as it accumulates wa's gain along the horizontal axis of Fig. 17a. This negative feedback dominance has the potential to close the gap between the walker and the pm average location. The biased Xwa change rate is falling at a locally maximum rate that corresponds to an inflection point on the trajectory of Xwa, where the smooth Xwa stock is rising at a locally maximum rate.

But the pm average walkers aim for is a moving target, so the walkers' transition along their distinct path groups **II** and **III** ends soon. Just a little before time t = 150, a sudden, discontinuous random shift in the walker's goal causes positive (reinforcing) feedback to dominate its deterministic motion. Its biased Xwa change rate now shows a positive slope on Fig. 17c as the walker begins to follow the pheromone molecules' random walk inside distinct path group **III**.

Figure 17
Shifting loop polarity (slp) along walker path groups II and III ($\rho$ = 50)

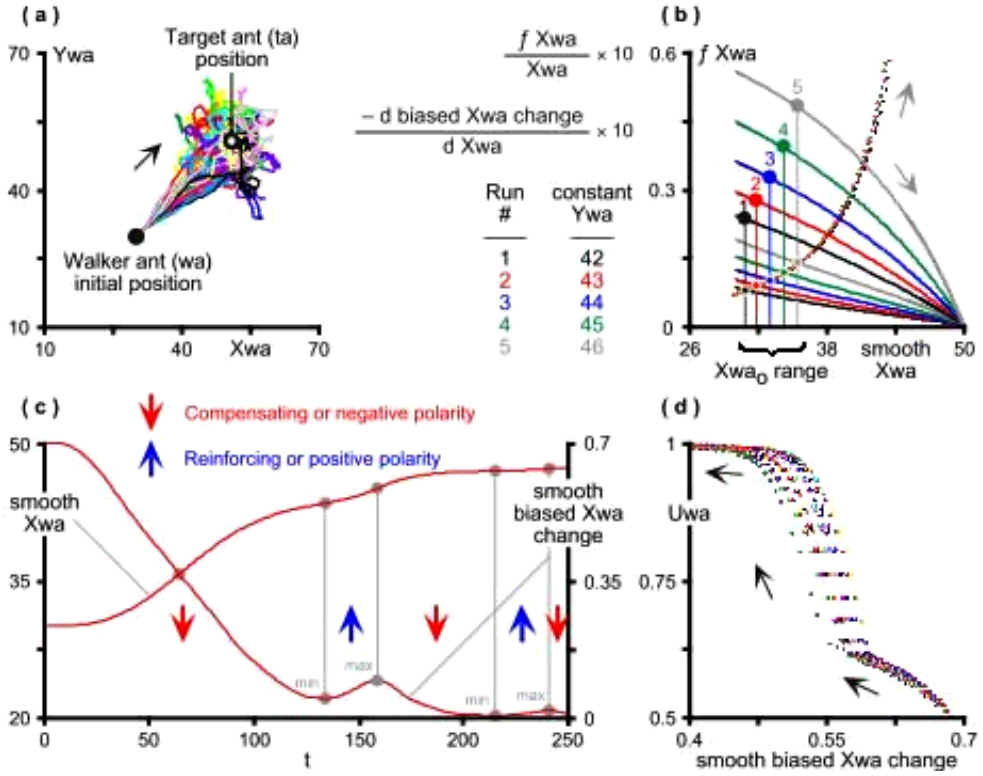


Inside walkers' biased motion region or path group **II**, uncertainty about their location rises orthogonally to their smooth biased Xwa change rate (Fig. 17d). The phase plot shows how walkers' initial guided motion toward the pm average accounts for at least 50 percent of location uncertainty at the macro level, i.e. Uwa = 0.5. Once the micro-level pheromones cause walkers' biased motion at the macro level, Uwa abandons its vertical climb and begins to rise concomitantly with the walkers' now decreasing smooth biased Xwa change. As walkers move toward what they perceive to be ta's location, the difference in X over the distance ratio inside the biased Xwa change (4.4) flow continues to drop nearly linearly, causing Uwa to rise at a declining rate. But once the walkers' biased motion begins to resemble the pheromones' continuous random walk, Uwa begins to rise faster again. By now, walkers are already far inside their path group **III**, where they behave just like the pm average. So uncertainty about their location rises fast, until Uwa saturates at Uwa = 1.

In walkers' transition along their distinct path groups **II** and **III**, the continuously moving pheromones at the micro level cause the macro-level agents to move orderly toward their perceived target. This orderly biased motion the pheromones trigger sequesters Uwa at the system's macro level. Within wa's path group **II**, as the walkers' smooth biased Xwa change decreases, it suppresses uncertainty about their location. The less walkers walk, the less they change their location, the smaller the uncertainty about their location becomes. But once inside path group **III**,

walkers fall pray to the pheromones' random motion, following them around deterministically. Uncertainty about their location now rises fast at the macro level, eventually matching uncertainty about pm average location at the micro level, i.e. Uwa = Upm = 1.

When inside walkers' perceptual radius, the micro-level pheromones reveal the target agent's existence and cause macro level agents to move orderly toward its location. This orderly, autopoietic behavior the pheromones trigger is what sequesters Uwa at the system's macro level.

**Conclusion**

Along with Prophet Sulayman's armies, the Qur'an mentions the ants' advanced communications system (Yahya, 2000). Here is the verse:

> Then, when they reached the valley of the ants, an ant said: 'Ants! Enter your dwellings so that Sulayman and his troops do not crush you unwittingly' (Surat an-Naml: 18).

Scientific research confirms the incredible communications network among these creatures. Using system dynamics to play with the ants and to understand complex, adaptive, self-organizing systems means looking at autopoietic processes causally, as opposed to merely at entropy measures. This model also replicated parts of Parunak & Brueckner's (2001) results. Despite its present inability to tag undifferentiated agents' attributes (Scholl 2001), the system dynamics method and software helps to understand exactly how CASOS' circular or feedback-loop relations produce nonlinear dynamics spontaneously out of their local interactions. As shifting loop polarity (slp) determines system behavior (Richardson 1995), distributed control leads positive feedback relations to explosive growth, which ends when all dynamics has been absorbed into an attractor, leaving the system in a stable, negative feedback state.

In addition to replicating parts of Parunak & Brueckner's (2001) results, the model reconfirms that the larger the random perturbations (noise) that affect a system, the more quickly it will self-organize to produce order. Replacing the if-then-else statements of Table 4 with a graphical table function (gtf) does not change the dynamics much, but does increase the number of loops in the wa sector from six to eight. Another variant entails letting walkers random-walk continuously, just like the pheromones do, even while these walkers chase pheromones. That reduces the wa sector loops from six to four and brings the model closer to what Parunak & Brueckner (2001, p. 125) see as "most realistic" behavior in their multi-agent CASOS study. But then it becomes impossible to separate the walkers' randomness from the pheromones'.

Assessing slp separately in walkers' transition, first between their distinct path groups **I** and **II**, and then again between groups **II** and **III**, helps explain the dynamics of the relation between walkers' biased motion rate and the macro-level uncertainty Uwa (lower left panel of Fig. 14). When walkers abandon their random walk to go meet their target, then the relation between their biased motion and Uwa becomes positive (Fig. 16d). However, when they deterministically follow the Brownian motion of the pheromones their target emits, then the same relation turns negative (Fig. 17d). In the first case, the walkers change their location under reinforcing or positive feedback (Fig. 16c). In the second case, they change their location under compensating or negative feedback (Fig. 17c). In both cases, Uwa rises because the walkers' location changes.

It is interesting to see, however, that as agents move from random disorder to autopoietic order with deterministic rules (Fig. 16a), then it is positive feedback that causes the relation between their rate of motion and location uncertainty to become positive (Fig. 16d). Conversely, when agents move, again deterministically, from static order to random disorder, then it is negative feedback that causes the relation between their rate of motion and location uncertainty to become negative (Fig. 17d).

In business, Williams (2002) sees a trend toward more customer intimacy in systems for personalization and communities of interest. This trend does not necessarily imply emergence, but one example of it, *eBay*, is an excellent business example of emergent behavior creating CASOS communities of interest. Another example is Bussmann & Schild's (2000) auction-based, self-organizing manufacturing control. *DaimlerChrysler* is evaluating this approach as a bypass to its existing manufacturing line. Performance tests demonstrate the industrial feasibility and benefits of self organization. And let's not forget the *Star Trek*-inspired Intelligent Room (Hanssens et al. 2002), which is changing what it means to use a computer. Rather than view a computer as a stand-alone box good only for word processing or e-mail, MIT's Intelligent Room is embedding computers in ordinary environments so that people can interact with them the way they do with other people, by speech, gesture, movement, affect and context.

In the context of practical CASOS action, Rough (1997) argues that CASOS facilitators must elicit and sustain breakthrough change processes, whether in persons, groups or organizations. Rather than trying to explain or to order what is needed, the facilitator attends to the change process and trusts that things will self-organize. The mechanistic paradigm we live in makes CASOS changes seem like magic. To understand CASOS facilitation, one must recognize the difference between managed change and self-organizing change. Rough's (1997) CASOS application examples include: (a) new insights where problems are spontaneously solved, (b) changes of heart where the trust level shifts and adversaries become friends, (c) a shift from dependency to empowerment, (d) a change of management style, from control to self-management and (e) people discovering what they really want instead of what they thought they wanted.

CASOS metaphors are good as far as they provide a springboard for discussion about the possibilities that emerge when combining physical and social sciences. To benefit from them, however, business managers and researchers must preserve CASOS rigor. System dynamics helps to explain why and to see exactly how CASOS generate their magnificent patterns; how CASOS structure causes autopoietic behavior. System dynamics perhaps can help articulate an interdisciplinary, posthumanist CASOS theory that shifts between contradictory elements in old and new sciences. But that may require distributed control among researchers themselves...

## References


Bonabeau, E.; Dorigo, M. & Theraulaz, G. (1999) *Swarm Intelligence: From Natural to Artificial Systems*. New York, NY: Oxford University Press.

Bussmann, S. & Schild, K. (2000) 'Self-organizing manufacturing control: An industrial application of agent technology. In *Proceedings of the 4th International Conference on Multi-Agent Systems*, Boston, MA: 10-12 July.

Forrester, J.W. (1958) 'Industrial dynamics: A major breakthrough for decision makers', *Harvard Business Review* 36(4): 37-66.

Georgantzas, N.C. (2001a) 'Self-organizing systems (SOS)', in M. Warner (Ed.), *International Encyclopedia of Business and Management* (2nd ed.). London, UK: Thomson Learning, 5792-5806.

Georgantzas, N.C. (2001b) 'Virtual enterprise networks: The fifth element of corporate governance', *Human Systems Management*, 20(3): 171-188.

Georgantzas, N. C. & W. Acar (1995) *Scenario-driven planning: Learning to manage strategic uncertainty*. Westport, CT: Greenwood.

Hanssens, N., Kulkarni, A., Tuchida, R. & Horton, T. (2002) *Building Agent-Based Intelligent Workspaces*. Cambridge, MA: MIT, Artificial Intelligence Lab.

Hayes, B. (1999) 'Computational creationism', *American Scientist* 87(5): 392-396.

Heylighen, F. (1999) 'The science of self-organization and adaptivity', in N.G. Basov et al., Eds. *Encyclopedia of Life Support Systems*. Paris, France: UNESCO-EOLSS Publishers.

Hock, D. (1998) 'Throwing away the mould', *CAmagazine* (Nov.): 40-41.

Holland, J. (1997) *Emergence: From chaos to order*. Redwood City, CA: Addison-Wesley.

Kauffman, S. (1995) *At home in the universe: The search for the laws of self-organization and complexity*. New York, NY: Oxford University Press.
Kugler, P.N. & Turvey, M.T. (1987) *Information, Natural Law, and the Self-Assembly of Rhythmic Movement*. New York, NY: Lawrence Erlbaum.
Lorenz, E. N. (1963) 'Deterministic nonperiodic flow', *Journal of the Atmospheric Sciences* 20(2): 130-141.
Morgan, G. (1993) *Imaginization: New mindsets for seeing, organizing, and managing*. San Francisco, CA: Berrett-Koehler.
Ormerod, P. (1999) *Butterfly economics: A new general theory of social and economic behavior*. New York, NY: Pantheon Books.
Parunak, H.V.D. (1997) 'Go to the ant: Engineering principles from natural agent systems', *Annals of Operations Research*, 75:69-101.
Parunak, H.V.D. & Brueckner, S. (2001) 'Entropy and self-organization in multi-agent systems', in *Proceedings of the International Conference on Autonomous Agents*, May 28-Jun. 1, Montreal, Canada: 124-130. Available online: http://www.anteaters.net/~sbrueckner/publications/2001/agents01ent.pdf.
Parunak, H.V.D. & Brueckner, S. (2000) 'Ant-like missionaries and cannibals: Synthetic pheromones for distributed motion control', in *Proceedings of the Fourth International Conference on Autonomous Agents*: 467-474.
Petzinger, T.J. (1997) 'Self-organization will free employees to act like bosses', *The Wall Street Journal* (3 Jan.).
Prigogine, I. & I. Strengers (1984) *Order out of chaos.* New York, NY: Bantam Books.
Richardson, G.P. (1995) 'Loop polarity, loop dominance, and the concept of dominant polarity', *System Dynamics Review* 11(1):67-88.
Richardson, G.P. & D.F. Andersen, Eds. (1988) *System Dynamics Review: Special Issue on Chaos*. Cambridge, MA: System Dynamics Group, MIT.
Richmond, B, (1980) 'A new look at an old friend', *Plexus*, Hanover, NH: Dartmouth College.
Richmond, B. et al. (2001) *iThink Analyst* 7: *The power to understand!* Hanover, NH: High Performance Systems, Inc.
Robertson, R. and A. Combs (Eds) (1995) *Chaos Theory in Psychology and the Life Sciences*. Mahwah, NJ: Lawrence Erlbaum.
Rough, J. (1997) 'Dynamic facilitation and the magic of self-organizing change', *Association for Quality and Participation* (June): http://www.tobe.net/papers/facilitn.htm.
Scholl, H.J. (2001) 'Looking across the fence: Comparing findings from system dynamics modeling efforts with those of other modeling techniques', in *Proceedings of the 19th International Conference of the System Dynamics Society*, 23-27 July, Atlanta, GA: 134.
Senge, P. et al. (1994) *The Fifth Discipline FIELDBOOK: Strategies and tools for building a learning organization*. New York, NY: Doubleday Currency.
Shannon, C.E. & Weaver, W. (1949) *The Mathematical Theory of Communication.* Urbana, IL: University of Illinois.
Sterman, J. D. (2000) *Business dynamics: Systems thinking and modeling for a complex world.* Boston, MA: Irwin McGraw-Hill.
Tribus, M. & McIrvine, E.C. (1971) 'Energy and information', *Scientific American* 224(Sep.): 178–184.
Turner, F. (1997) 'Foreword: Chaos and social science', in R.A. Eve, S. Horsfall & M.E. Lee, Eds. *Chaos, complexity and sociology.* Thousand Oaks, CA: Sage, (pp. xi-xxvii).
Ueda, Y. (1992) 'Strange attractors and the origin of chaos', *Nonlinear Science Today* 2(2): 1-8.
Wheatley, M. J. (1996) 'The unplanned organization: Learning from nature's emergent creativity', *Noetic Sciences Review* (Spring, #37): 16-23.
Williams, J.D. (2002) 'Emergence', *Application Development Trends,* (May). Available online: http://www.adtmag.com/print.asp?id=6312.
Yahya, H. (2000) *The Miracle In The Ant* (Online). Available: http://www.harunyahya.org/Eng/ant/ant01.html.
Zeleny, M. (2000) 'New economy of networks', *Human Systems Management* 19(1): 1-5.
Zhabotinsky, A. M. (1973) 'Autowave processes in a distributed chemical system', *Journal of Theoretical Biology* 40: 45-61.

Back to the Top